# Deubiquitinase USP13 maintains glioblastoma stem cells by antagonizing FBXL14-mediated Myc ubiquitination

Xiaoguang Fang,[1] Wenchao Zhou,[1] Qiulian Wu,[1] Zhi Huang,[1] Yu Shi,[1,2] Kailin Yang,[1] Cong Chen,[1,2] Qi Xie,[1] Stephen C. Mack,[1] Xiuxing Wang,[1] Angel M. Carcaboso,[3] Andrew E. Sloan,[4,5] Gaoliang Ouyang,[6] Roger E. McLendon,[7] Xiu-wu Bian,[2] Jeremy N. Rich,[1,5] and Shideng Bao[1,5]

[1]Department of Stem Cell Biology and Regenerative Medicine, Lerner Research Institute, Cleveland Clinic, Cleveland, OH 44195
[2]Institute of Pathology and Southwest Cancer Center, Southwest Hospital, Key Laboratory of Tumor Immunopathology, Ministry of Education of China, Chongqing 400038, China
[3]Preclinical Therapeutics and Drug Delivery Research Program, Fundacio Sant Joan de Deu, 08950 Barcelona, Spain
[4]Department of Neurological Surgery, University Hospitals and [5]Case Comprehensive Cancer Center, Case Western Reserve University School of Medicine, Cleveland, OH 44106
[6]The State Key Laboratory of Cellular Stress Biology, School of Life Sciences, Xiamen University, Xiamen 361102, China
[7]Department of Pathology, Duke University Medical Center, Durham, NC 27710

**Glioblastoma is the most lethal brain tumor and harbors glioma stem cells (GSCs) with potent tumorigenic capacity. The function of GSCs in tumor propagation is maintained by several core transcriptional regulators including c-Myc. c-Myc protein is tightly regulated by posttranslational modification. However, the posttranslational regulatory mechanisms for c-Myc in GSCs have not been defined. In this study, we demonstrate that the deubiquitinase USP13 stabilizes c-Myc by antagonizing FBXL14-mediated ubiquitination to maintain GSC self-renewal and tumorigenic potential. USP13 was preferentially expressed in GSCs, and its depletion potently inhibited GSC proliferation and tumor growth by promoting c-Myc ubiquitination and degradation. In contrast, overexpression of the ubiquitin E3 ligase FBXL14 induced c-Myc degradation, promoted GSC differentiation, and inhibited tumor growth. Ectopic expression of the ubiquitin-insensitive mutant T58A–c-Myc rescued the effects caused by FBXL14 overexpression or USP13 disruption. These data suggest that USP13 and FBXL14 play opposing roles in the regulation of GSCs through reversible ubiquitination of c-Myc.**

## INTRODUCTION

Glioblastoma multiforme (GBM) is the most common and malignant primary brain tumor with an extremely poor prognosis. Despite the implementation of aggressive therapies including surgery, radiation, and chemotherapy, the median survival of GBM patients remains <16 mo (Stupp et al., 2005, 2009; Wen and Kesari, 2008), underscoring the challenge to treat this fatal cancer. GBM displays remarkable intratumoral heterogeneity as demonstrated by glioma cells that form a tumor hierarchy of cells with diverse tumorigenic potential (Chen et al., 2010; Charles et al., 2012; Kreso and Dick, 2014). Glioma stem cells (GSCs) reside at this hierarchical apex and have been shown to contribute to the process of tumor initiation, malignant progression, therapeutic resistance, and tumor recurrence (Hemmati et al., 2003; Singh et al., 2004; Bao et al., 2006a; Lee et al., 2006; Liu et al., 2006; Piccirillo et al., 2006; Calabrese et al., 2007; Gilbertson and Rich, 2007; Chen et al., 2012). Similar to neural progenitor cells (NPCs), GSCs display the capacity of self-renewal and multilineage differentiation (Singh et al., 2004; Lee et al., 2006; Cheng et al., 2013; Suvà et al., 2014; Yan et al., 2014). The stem cell–like properties and tumorigenic potential of GSCs are maintained by a set of core stem cell transcription factors (SCTFs) such as SOX2 and c-Myc. These key stem cell factors are tightly regulated by both transcriptional control and posttranslational modifications. However, the mechanisms by which these core SCTFs are regulated at posttranslational levels in GSCs remain poorly understood. A comprehensive understanding of posttranslational control programs such as ubiquitination and deubiquitination of these key SCTFs, including c-Myc, in GSCs may facilitate the development of new therapeutic strategies to significantly improve GBM treatment.

c-Myc is a well-known basic helix-loop-helix transcription factor that controls expression of a large number of critical genes (Blackwood and Eisenman, 1991; Dang, 2012; Nie et al., 2012). c-Myc is highly expressed in ∼70% of human cancers and correlates with poor prognosis in patients (Varley et al., 1987; Field et al., 1989; Cole and Cowling,

Correspondence to Shideng Bao: baos@ccf.org; or Jeremy N. Rich: richj@ccf.org

Abbreviations used: bFGF, basic fibroblast growth factor; EGF, epidermal growth factor; GBM, glioblastoma multiforme; GFAP, glial fibrillary acidic protein; GSC, glioma stem cell; HA, hemagglutinin; IB, immunoblot; IHC, immunohistochemical; IP, immunoprecipitation; LC-MS, liquid chromatography mass spectrometry; NPC, neural progenitor cell; NSTC, nonstem tumor cell; PDX, patient-derived xenograft; PI, propidium iodide; SCTF, stem cell transcription factor; shNT, nontargeting shRNA; SVZ, subventricular zone; TUNEL, terminal deoxynucleotidyl transferase deoxyuridine triphosphate nick-end labeling.



The Rockefeller University Press $30.00
J. Exp. Med. 2017 Vol. 214 No. 1 245–267
https://doi.org/10.1084/jem.20151673

2008; Delmore et al., 2011; Lin et al., 2012). In human brain cancers including GBMs, the c-Myc gene is dysregulated, causing elevated expression of c-Myc to promote tumor progression (Trent et al., 1986; Wasson et al., 1990; Wang et al., 2008; Zheng et al., 2008). In addition, c-Myc is a critical transcriptional factor for maintaining GSC self-renewal and tumorigenic potential (Wang et al., 2008). Disruption of c-Myc by shRNA diminished glioma formation in mice (Wang et al., 2008). We have previously demonstrated that the elevated expression of c-Myc in GSCs at the transcriptional level is regulated by another SCTF, zinc finger X-chromosomal protein (Fang et al., 2014). How c-Myc protein is regulated at the posttranslational level in GSCs remains unclear. Studies of other cancer types have revealed several ubiquitin E3 ligases, including Fbw7, Skp2, and HectH9, that target c-Myc protein for proteasome-mediated degradation (von der Lehr et al., 2003; Yada et al., 2004; Adhikary et al., 2005). Similarly, deubiquitinases USP28, USP36, and USP37 have been shown to stabilize c-Myc protein in some types of cancers (Popov et al., 2007; Pan et al., 2015; Sun et al., 2015). These studies suggest that the ubiquitination and deubiquitination regulation of c-Myc may be cell context dependent. Thus, we sought to identify the key ubiquitin E3 ligases and deubiquitinases of c-Myc in GSCs and investigate their biological roles in controlling the stem cell–like properties of GSCs. In addition, elucidation of the posttranslational regulatory mechanisms of c-Myc may offer new insights into the maintenance of GSC tumorigenic potential and reveal novel GSC-specific therapeutic targets. In this study, we found that c-Myc protein stability is contrarily regulated by the deubiquitinase USP13 and the ubiquitin E3 ligase FBXL14 (F-box and leucine-rich repeat protein 14) in patient-derived GBM cells.

Deubiquitinase USP13 is a member of the cysteine-dependent protease superfamily (Reyes-Turcu et al., 2006). USP13 functions as a ubiquitin-specific enzyme by cleaving the K48-linked polyubiquitin chain off protein substrate to reverse ubiquitin-mediated protein degradation (Clague and Urbé, 2010). During the ER-induced cell cycle regulation, USP13 is recruited by nuclear ubiquitin-recognition protein Ufd1 to counteract APC/$C^{Cdh1}$-mediated ubiquitination of Skp2 (Chen et al., 2011). In melanoma cells, USP13 attenuates the autodegradation of Siah2, a RING (really interesting new gene) finger family E3 ubiquitin ligase (Scortegagna et al., 2011). In addition, USP13 has been shown to promote melanoma tumor growth by stabilizing the microphathalmia-associated transcription factor (Zhao et al., 2011). However, the functional significance of USP13 in regulating the GSC phenotype has not been defined.

FBXL14, which contains 11 leucine-rich repeats and an F-box motif, is one of the RING family ubiquitin E3 ligases (Jin et al., 2004). FBXL14 plays an important role in the formation of stem cell factor complexes by binding to Skp1, cullin, and RBX1 (Jin et al., 2004; Nakayama and Nakayama, 2006; Metzger et al., 2012). Deletion of *FBXL14* was found to associate with the neurological disorders (Abdelmoity et al., 2011). FBXL14 is also essential for vertebrate axis formation in zebrafish (Zheng et al., 2012). As a tumor suppressor, FBXL14 has been shown to control Snail1, an essential regulator of the epithelial-mesenchymal transition under hypoxia condition. Its homologue Ppa also regulates epithelial-mesenchymal transition factors including Twist, Snail, Slug, and Sip1 in the neural crest development of *Xenopus laevis* (Viñas-Castells et al., 2010; Lander et al., 2011). However, the role of FBXL14 in regulating GSC transcription factors has not been elucidated. To define the posttranslational regulation of c-Myc in GSCs, we identified FBXL14 and USP13 as a pair of opposing ubiquitin E3 ligase and deubiquitinase that control c-Myc protein stability in glioma cells. We demonstrate that USP13-mediated deubiquitination counteracts FBXL14-promoted ubiquitination to stabilize c-Myc protein and maintain GSC phenotype and tumorigenic potential. This discovery suggests that deubiquitinase USP13 may represent a potential therapeutic target for GBM through perturbation of oncogenic c-Myc stability.

## RESULTS

### USP13 and FBXL14 interact with c-Myc in glioma cells

To identify potential ubiquitin ligases and deubiquitinases that regulate c-Myc protein stability in glioma cells, we interrogated c-Myc–interacting proteins in glioma cells derived from GBM tumors. GSCs and matched nonstem tumor cells (NSTCs) were isolated from primary GBMs or patient-derived xenografts (PDXs) through cell sorting ($CD15^+$/$CD133^+$ for GSCs and $CD15^-$/$CD133^-$ for NSTCs) as previously described (Son et al., 2009; Guryanova et al., 2011; Cheng et al., 2013; Zhou et al., 2015). Sorted GSCs were functionally characterized by three assays including self-renewal (in vitro serial neurosphere formation), multipotent differentiation (induction of multilineage differentiation in vitro), and tumor initiation (in vivo limiting dilution tumor formation assay), as previously described (Lee et al., 2006; Guryanova et al., 2011; Cheng et al., 2013; Zhou et al., 2015). Immunoprecipitation (IP) and mass spectrometry were used to identify c-Myc–interacting proteins in PDX-derived glioma cells. Specifically, Flag-tagged c-Myc was introduced into GSCs (T387) through lentiviral infection. Tandem pull-down of exogenous c-Myc was performed through sequential immunopurification using the affinity resins against the Flag tag and then the Myc epitope in the partially differentiated GSCs that were induced by serum for a short time (2 d). The purified c-Myc complex was subjected to SDS-PAGE, and the interacting proteins in the complex were detected by silver staining (not depicted). Protein bands were excised from the gel and then analyzed by mass spectrometry to determine the identities of interacting proteins in the immunoprecipitated complex. As a positive indication, several known c-Myc–interacting proteins including Max and transformation-transcription domain–associated protein were detected in the complex (not depicted). Interestingly, we found two deubiquitinases including USP13 and three E3 ligases

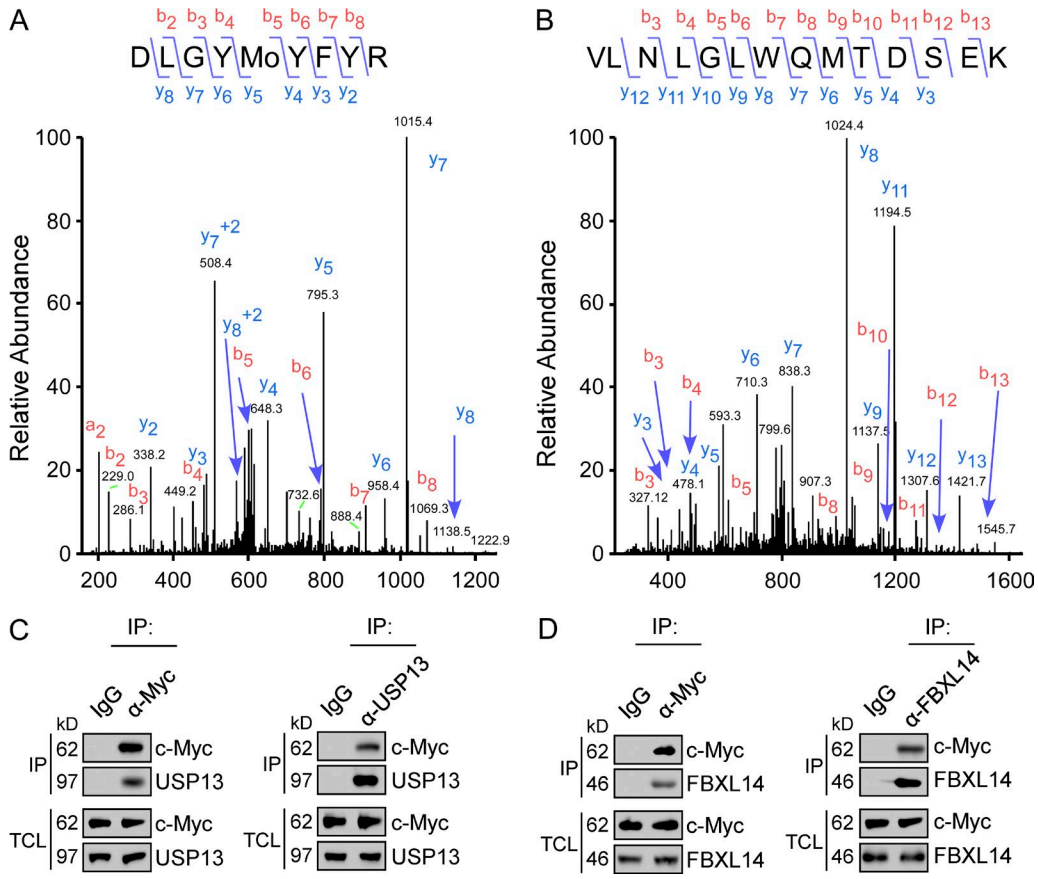


Figure 1. **Identification of USP13 and FBXL14 as c-Myc–interacting proteins in glioma cells.** (A and B) Identification of USP13 peptide (A) and FBXL14 peptide (B) in the c-Myc–interacting proteins by mass spectrometry analysis. c-Myc–interacting proteins were immunoprecipitated from partially differentiated GSCs (T387) that were induced by serum for a short time (2 d). Protein complexes were digested with trypsin before analysis by LC-MS. Ubiquitin-specific protease 13 (USP13) and the F-box/LRP-repeat protein 14 (FBXL14) were identified in LC-MS analysis by the peptides covering the protein sequence. The mass spectrometry spectra for the USP13 peptide DLGYMoYFYR (A) and the FBXL14 peptide VLNLGLWQMTDSEK (B) are shown. (C and D) Co-IP analyses of protein interaction between endogenous c-Myc and USP13 (C) or FBXL14 (D) in partially differentiated GSCs (T387) induced by serum for a short time (2 d). Cell lysates were immunoprecipitated with specific antibodies against c-Myc, USP13, or FBXL14. The co-IP complexes and total cell lysates were analyzed by IB with antibodies against c-Myc and USP13 or FBXL14. TCL, total cell lysate.

including FBXL14 in the IP complex (Fig. 1, A and B; and not depicted). To determine which deubiquitinases and E3 ligases play a role in regulating c-Myc protein stability in glioma cells, we performed quantitative PCR to determine the gene expression profiles of the identified deubiquitinases and E3 ligases between GSCs and matched NSTCs from GBM tumors. We found that USP13 is preferentially expressed in GSCs and FBXL14 is elevated in NSTCs (not depicted). As c-Myc protein level is up-regulated in GSCs and down-regulated in NSTCs, we reasoned that preferential expression of the deubiquitinase USP13 in GSCs and the ubiquitin E3 ligase FBXL14 in NSTCs could regulate c-Myc protein levels through ubiquitination and deubiquitination.

The interaction between c-Myc and USP13 or FBXL14 was validated in HEK293 cells coexpressing c-Myc and Flag-tagged USP13 or FBXL14. Co-IP experiments showed that either USP13 or FBXL14 was pulled down by anti-Myc antibody (not depicted). Likewise, c-Myc was coimmunoprecipitated with USP13 or FBXL14 by anti-Flag antibody (not depicted). To further confirm the interaction between endogenous c-Myc and USP13 or FBXL14 in GSCs, c-Myc was immunoprecipitated from cell lysate of partially differentiated GSCs that were induced by serum acutely (2 d). Both USP13 and FBXL14 were detected in the complex precipitated by anti–c-Myc antibody (Fig. 1, C and D). Consistently, c-Myc was coprecipitated by the anti-USP13 or the anti-FBXL14 antibody (Fig. 1, C and D). These results demonstrate that c-Myc interacts with USP13 and FBXL14 in glioma cells, indicating that deubiquitinase USP13 and the ubiquitin E3 ligase FBXL14 are potential regulators of c-Myc protein stability in GBM.

## USP13 is preferentially expressed in GSCs in GBMs

As USP13 is a deubiquitinase, the interaction between USP13 and c-Myc led us to hypothesize that USP13 may stabilize c-Myc protein in GSCs through deubiquitination. The prefer-

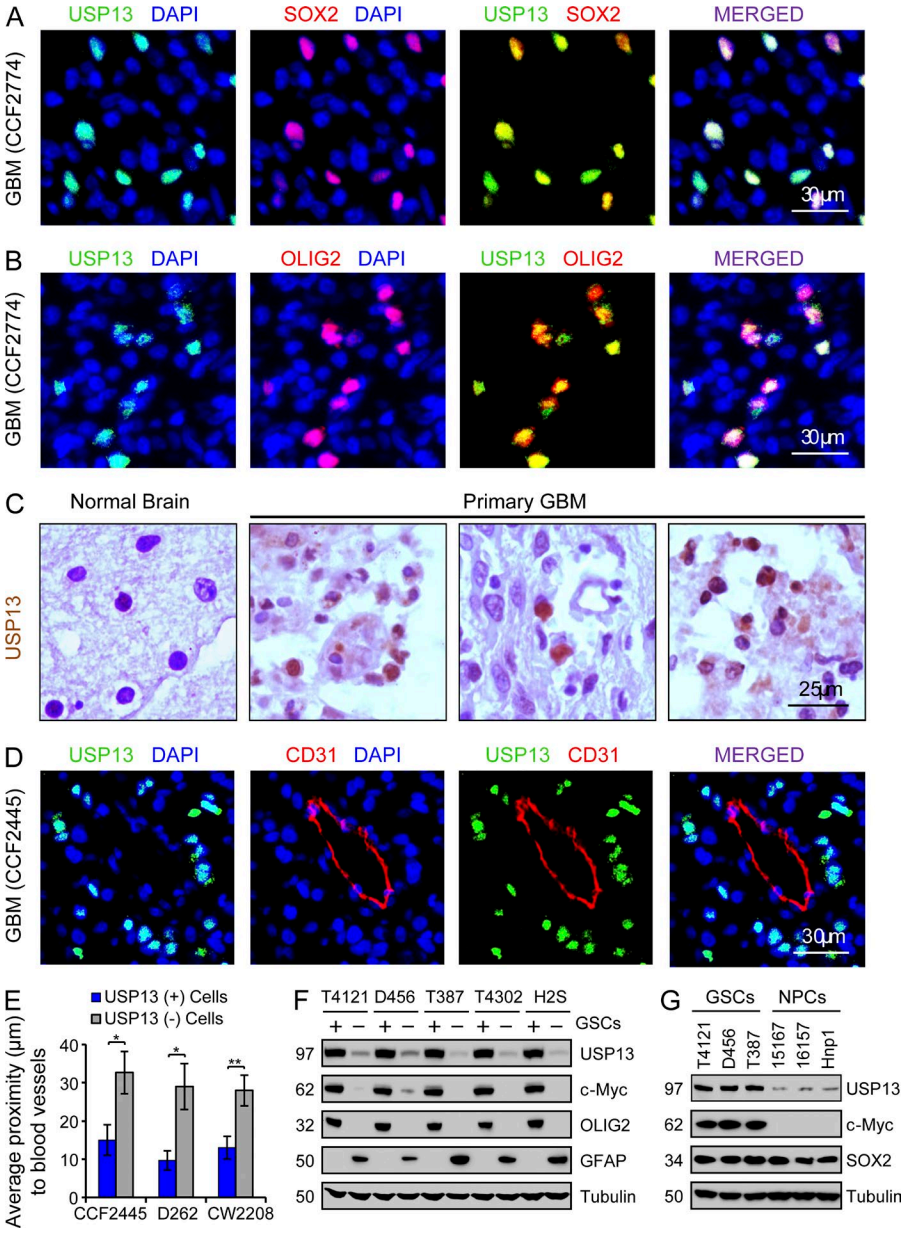


Figure 2. **USP13 is preferentially expressed in GSCs in human GBMs.** (A and B) Immunofluorescent staining of USP13 and the GSC marker SOX2 (A) or OLIG2 (B) in a primary GBM. Frozen sections of GBM (CCF2774) were coimmunostained with specific antibodies against USP13 (green) and the GSC marker SOX2 or OLIG2 (red) and then counterstained with DAPI (blue) to show nuclei. USP13 is coexpressed in the glioma cells expressing the GSC markers. (C) IHC staining of USP13 (brown) in human normal brain tissue and primary GBMs. Tissue sections were counterstained with hematoxylin to mark nuclei. USP13 is expressed in a fraction of cancer cells in GBMs but not expressed in the normal brain. (D) Immunofluorescent staining of USP13 and the endothelial marker CD31 in a primary GBM. Frozen sections of GBM (CCF2445) were coimmunostained with specific antibodies against USP13 (green) and CD31 (red) and then counterstained with DAPI (blue) to show nuclei. USP13 cells are localized in the perivascular niche. (E) The mean proximities of USP13-positive cells (+) and USP13-negative cells (–) to blood vessels in primary GBMs were statistically analyzed in three cases of human GBMs (CCF2445, D262, and CW2208). The USP13 (+) cells were significantly more proximal to blood vessels than USP13 (–) cells. Data are mean ± SD. $n = 3$. *, $P < 0.05$; **, $P < 0.01$. Student's $t$ test was used to assess the significance. Data are from three independent experiments. (F) IB analysis of USP13, c-Myc, OLIG2, and GFAP in GSCs (+) and matched NSTCs (–) isolated from five GBM tumors. OLIG2 and c-Myc are GSC markers, whereas GFAP is an astrocyte marker. (G) IB analysis of USP13, c-Myc, and SOX2 in GSC populations and human NPC lines. GSCs express more USP13 and c-Myc than normal NPCs. (F and G) Mass is shown in kilodaltons.

ential expression of USP13 in GSCs was validated in primary GBM tumors directly from patients and the isolated GSC populations derived from GBM xenografts. Coimmunofluorescent staining demonstrated that USP13 was preferentially expressed in the glioma cells expressing the GSC markers including SOX2 and OLIG2 and in human primary GBMs (Fig. 2, A and B), but USP13 is not expressed in the normal brain tissue adjacent to the tumor (not depicted). Immunohistochemical (IHC) staining confirmed that USP13 is differentially expressed in a fraction of cells in primary GBMs and PDXs but not in the adjacent normal brain tissues (Fig. 2 C and not depicted). Interestingly, USP13-expressing cells are proximal to blood vessels marked by CD31 staining in primary GBMs (Fig. 2, D and E), but USP13 is not expressed in normal brain tissues even in areas around blood vessels (not depicted), which is consistent with the fact that GSCs are often localized in perivascular niches (Calabrese et al., 2007; Li et al., 2009; Guryanova et al., 2011). In addition, immunoblot (IB) and RT-PCR analyses further validated that USP13 and the GSC markers including c-Myc, SOX2, and OLIG2 were preferentially expressed in the isolated GSC populations from GBM surgical specimens or xenografts (Fig. 2 F and not depicted). Immunofluorescent staining confirmed preferential expressions of USP13 and the GSC marker SOX2 or c-Myc in sorted GSCs relative to matched NSTCs (not depicted). Collectively, these data demonstrate that USP13 is preferentially expressed in GSCs in human GBM tumors.

As GSCs share similar properties with NPCs, we then examined USP13 expression patterns in NPC lines and the

subventricular zone (SVZ), which is enriched with NPCs. IB analysis showed that USP13 and c-Myc levels in NPCs were much lower than those in GSCs (Fig. 2 G). Immunofluorescence staining confirmed that USP13 was rarely expressed in NPCs (not depicted). As NPCs are typically identified as $SOX2^+$ cells in the SVZ, we performed coimmunofluorescent staining of SOX2 with USP13 or c-Myc in SVZs from mouse brains. Consistently, expression levels of USP13 and c-Myc are low in $SOX2^+$ NPCs in normal brain (not depicted). Collectively, these data demonstrate that USP13 is differentially expressed in GSCs relative to NSTCs and NPCs, suggesting that USP13 is a potential GSC marker and GSC-specific therapeutic target.

### Targeting USP13 reduces c-Myc protein levels and impairs GSC maintenance

As USP13 is preferentially expressed in GSCs and USP13 protein levels gradually decreased during GSC differentiation (Fig. 3 A), we proposed that USP13 may play an important role in the maintenance of GSCs. To elucidate the functional significance of USP13 in maintaining the GSC phenotype, we examined the effects of USP13 knockdown on c-Myc protein level, GSC growth, and tumorsphere formation. Disrupting USP13 by lentiviral-mediated shRNA (shUSP13-50 or shUSP13-52) in GSCs reduced USP13 protein by 90%, which also induced a rapid and marked reduction of c-Myc protein (Fig. 3 B). Immunofluorescence confirmed that c-Myc protein level decreased after USP13 knockdown (not depicted), whereas c-Myc mRNA level remained unchanged as demonstrated by RT-PCR analysis (not depicted). In contrast, overexpression of USP13 (Flag-USP13) increased c-Myc protein levels in GSCs (Fig. 3 C). Moreover, treatment with a proteasome inhibitor blocked the c-Myc loss caused by USP13 knockdown (not depicted), but overexpression of USP13 delayed c-Myc turnover in the presence of cycloheximide (not depicted), suggesting a critical role of USP13 in preventing proteasomal degradation of c-Myc in GSCs. As c-Myc is crucial for the maintenance of GSCs, down-regulation of c-Myc by USP13 disruption negatively impacts GSC function. A tumorsphere formation assay demonstrated that disrupting USP13 by shRNA significantly reduced GSC tumorsphere formation as indicated by decreased size and number of GSC tumorspheres (Fig. 3, D–F). In addition, USP13 disruption significantly reduced GSC proliferation (Fig. 3, G and H) but showed little effects on NSTCs and NPCs (not depicted). Flow cytometry analysis with FITC-labeled anti–annexin V antibody indicated that disrupting USP13 significantly increased apoptosis of GSCs (Fig. 3, I and J). Furthermore, the expressions of downstream target genes of c-Myc were significantly reduced after USP13 disruption by shRNA (Fig. 3 K), supporting the functional regulation of c-Myc protein stability by USP13 in GSCs. Collectively, these data demonstrate that USP13 is required for the proper regulation of self-renewal and proliferation of GSCs through stabilization of c-Myc protein.

### Disrupting USP13 abrogates GSC tumor growth

To determine the effect of USP13 disruption on GSC tumorigenic potential in vivo, we examined the tumor propagating capacity of GSCs transduced with USP13 shRNAs (shUSP13-50 or shUSP13-52) or nontargeting shRNA (shNT) control. The GSCs were also transduced with firefly luciferase, which allows monitoring of tumor growth in living animals by bioluminescent imaging. GSCs expressing luciferase and shUSP13 or shNT were transplanted into the brains of immunocompromised mice. Bioluminescent analysis showed that targeting USP13 by two independent shRNAs markedly impaired GSC tumor growth (Fig. 4, A and B). Mice sacrificed at day 21 demonstrated that GSCs transduced with shUSP13 either failed to form tumors or only harbored relatively small tumors, whereas the control group developed huge tumors in the mouse brains (Fig. 4 C). As a consequence, mice intracranially transplanted with the GSCs expressing shUSP13 survived significantly longer than the control group ($P < 0.001$; Fig. 4 D). In addition, IHC staining of Ki-67 and cleaved caspase 3 confirmed that USP13 disruption reduced c-Myc protein in the GSC-derived xenografts and led to a significant decrease in cell proliferation and an increase in cell apoptosis within the tumor (not depicted). To further confirm the clinical relevance of targeting USP13 in established GBM tumors, we applied the Tet-on inducible knockdown system to examine whether inducible disruption of USP13 by doxycycline affects the growth of established xenograft tumors and animal survival. In vitro analysis showed inducible disruption of USP13 in GSCs by 70% reduced c-Myc protein levels and inhibited GSC proliferation (Fig. 4, E and F). In vivo bioluminescent analysis confirmed that induced disruption of USP13 by doxycycline treatment significantly inhibited GSC tumor growth in mouse intracranial xenografts (Fig. 4, G and H). Furthermore, mice intracranially transplanted with GSCs expressing shUSP13 induced by doxycycline treatment survived significantly longer than the control mice (Fig. 4 I). Collectively, these data demonstrate that USP13 is required for maintaining the tumorigenic capacity of GSCs in vivo, indicating that targeting USP13 to disrupt GSCs may imply therapeutic potential.

### FBXL14 is preferentially expressed in nonstem glioma cells

As we identified that the ubiquitin E3 ligase FBXL14 also interacts with c-Myc in glioma cells, we speculated whether FBXL14 mediates ubiquitination of c-Myc for proteasomal degradation in NSTCs. IB analysis demonstrated that FBXL14 was highly expressed in NSTCs but showed significantly decreased expression in matched GSCs (Fig. 5 A). Coimmunofluorescent staining of FBXL14 with a stem cell marker (SOX2 or c-Myc) or differentiation marker (glial fibrillary acidic protein [GFAP] or TUJ1) confirmed that FBXL14 was preferentially expressed in NSTCs relative to matched GSCs (Fig. 5, B and C; and not depicted). During GSC differentiation, the expression of FBXL14 increased gradually in parallel

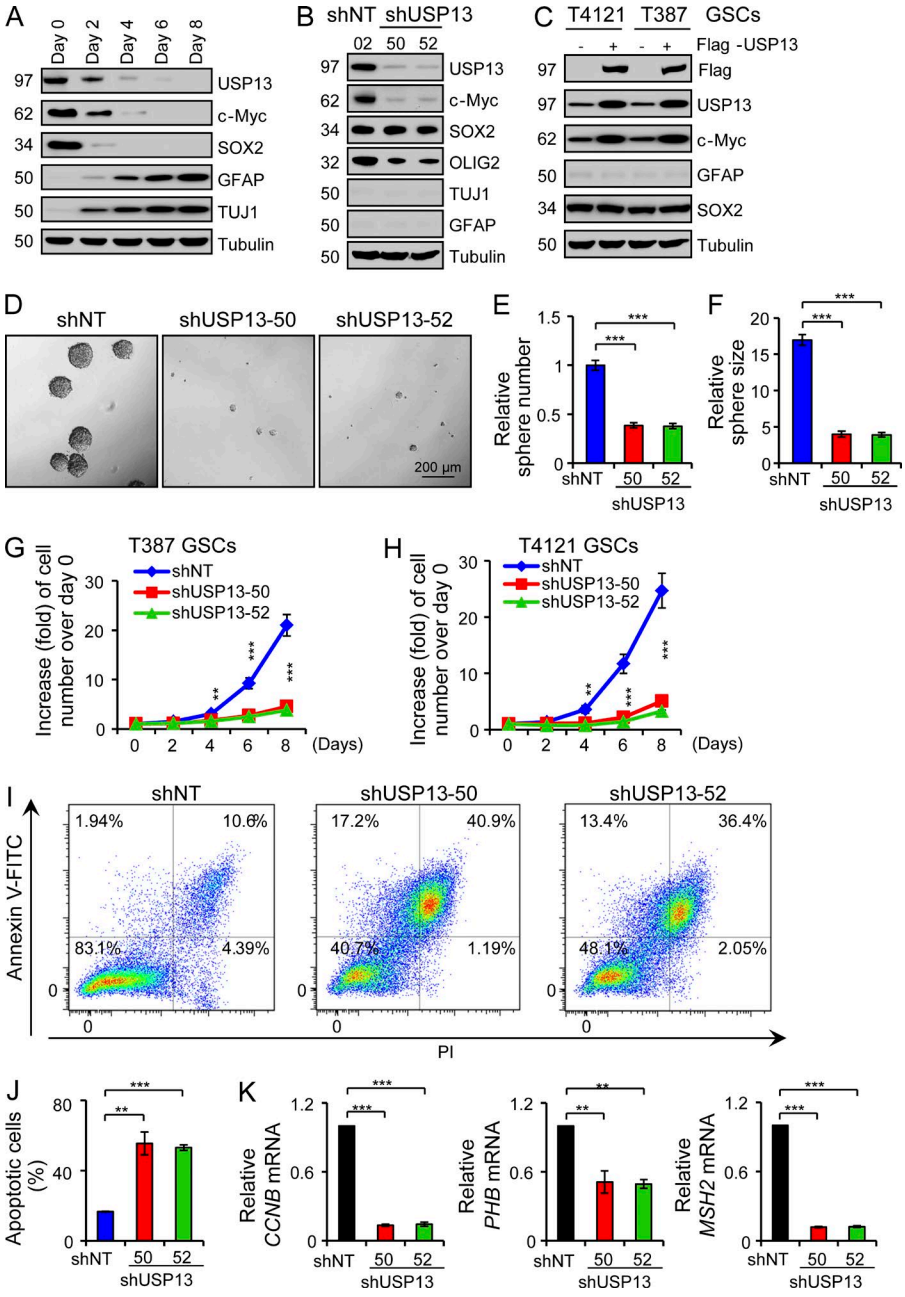


Figure 3. **Targeting USP13 disrupted the maintenance of GSCs.** (A) IB analysis of USP13, the GSC markers (c-Myc and SOX2), and the differentiation markers (GFAP and TUJ1) during serum-induced GSC differentiation. GSCs isolated from T4121 xenografts were cultured in DMEM containing 10% FBS to induce differentiation and harvested for IB analysis on the indicated days. USP13, c-Myc, and SOX2 gradually decreased, whereas the differentiation markers GFAP (for astrocytes) and TUJ1 (for neurons) increased during the differentiation. (B) IB analysis of USP13, c-Myc, SOX2, OLIG2, TUJ1, and GFAP in the GSCs (T387) transduced with USP13 shRNA (shUSP13-50 and shUSP13-52) or shNT (02) for 2 d. USP13 disruption by shRNA for a short time rapidly induced a dramatic decrease of c-Myc protein level in GSCs. (C) IB analysis of USP13, c-Myc, GFAP, and SOX2 in the GSCs transduced with Flag-USP13 expression or vector control through lentiviral infection in two GSC populations derived from T4121 and T387 xenografts. Forced expression of USP13 increased c-Myc protein levels in GSCs. (A–C) Mass is shown in kilodaltons. (D–F) The effect of USP13 knockdown on GSC tumorsphere formation. Disrupting USP13 by shUSP13-50 or shUSP13-52 impaired tumorsphere formation of GSCs (T387). (D) Representative images of GSC tumorspheres are shown. (E and F) Quantification showing that USP13 knockdown significantly reduced GSC tumorsphere number (E) and size (F). $n = 4$. (G and H) Growth curves of GSCs expressing shUSP13 or shNT control. GSCs derived from T387 xenograft (G) or T4121 xenograft (H) were transduced with shUSP13 (sh50 and sh52) or shNT and then measured for cell growth over a time course (day 0 to day 8). Disrupting USP13 significantly inhibited the growth of GSCs. $n = 6$. (I and J) Annexin V–FITC staining to detect apoptosis in GSCs expressing shUSP13 or shNT. GSCs (T387) were transduced with shUSP13 or shNT through lentiviral infection for 48 h, stained with annexin V-FITC and PI, and then analyzed by flow cytometry. (I) Representative FACS data are shown. The upper right dots represent late apoptotic cells (positive for both annexin V and PI). (J) Quantifications showing that disrupting USP13 significantly increased apoptosis of GSCs. $n = 3$. (K) RT-PCR analysis of expression of c-Myc downstream targets including cyclin B (*CCNB*), prohibitin (*PHB*), and DNA mismatch repair protein (*MSH2*) in the GSCs expressing shUSP13 (sh50 or sh52) or shNT. GSCs (T387) were transduced with shUSP13 shNT for 48 h through lentiviral infection, and the RNA samples were isolated for RT-PCR analysis with specific primers for *CCNB*, *PHB*, and *MSH2*. Disruption of USP13 also reduced expressions of c-Myc downstream targets in GSCs. $n = 3$. Data are mean ± SD. **, $P < 0.01$; ***, $P < 0.001$; shNT versus shUSP13. Student's *t* test was used to assess the significance. Data are from three independent experiments.

with the astrocyte marker GFAP and neuronal markers TUJ1 and MAP2 (Fig. 5 D). To further validate the preferential expression of FBXL14 in NSTCs in human primary GBMs in situ, we performed coimmunofluorescence of FBXL14 with a differentiated cell marker (MAP2 or GFAP) or a stem cell marker (SOX2) on GBM tumor sections. We confirmed that FBXL14 was preferentially expressed in glioma cells expressing the astrocyte marker (GFAP) or the neural marker (MAP2) but not in GSCs expressing SOX2 in human primary GBMs (Fig. 5, E–G). Interestingly, FBXL14 expres-

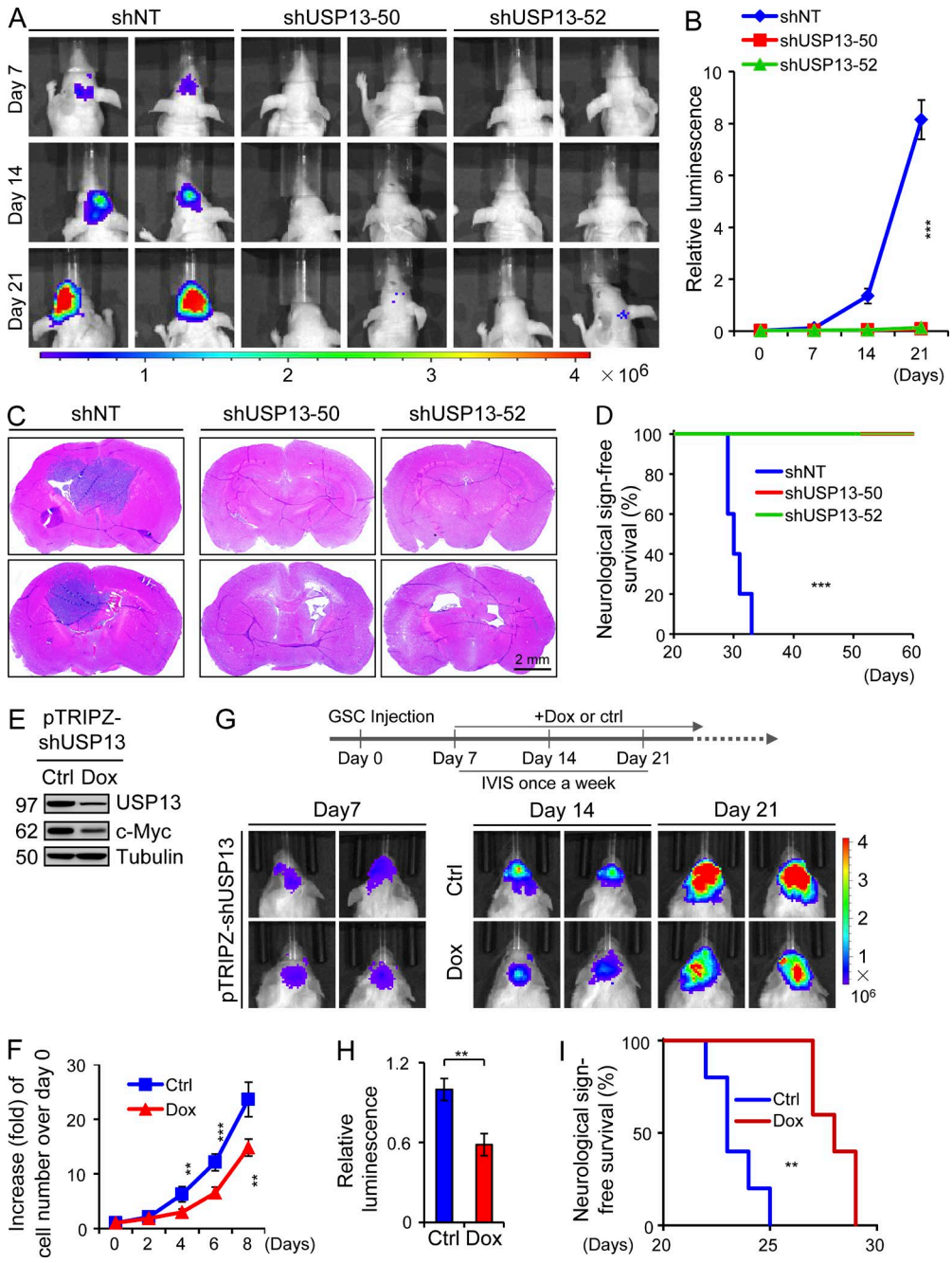


Figure 4. **Disrupting USP13 inhibited GSC tumor growth and prolonged animal survival.** (A and B) In vivo bioluminescent imaging of GBM xenografts derived from luciferase-labeled GSCs expressing shUSP13 or shNT control. GSCs (T387) were transduced with shUSP13 (shUSP13-50 or shUSP13-52) or shNT and then transplanted into brains of immunocompromised mice ($5 \times 10^3$ cells per animal). Mice bearing the intracranial xenografts were monitored after GSC transplantation. (A) Representative bioluminescent images at the indicated days are shown. (B) Quantification of bioluminescence indicated that disrupting USP13 significantly attenuated GSC tumor growth in mouse brains. $n = 5$. ***, $P < 0.001$; shNT versus shUSP13. Student's $t$ test was used to assess the significance. Five mice per group were used. (C) Representative images of mouse brain cross sections from mice intracranially implanted with the GSCs transduced with shUSP13 or shNT. GSCs (T387) were transduced with shUSP13 or shNT through lentiviral infection for 48 h and then transplanted into mouse brains. Cross sections (hematoxylin and eosin stained) of the mouse brains harvested on day 21 after injection are shown. (D) Kaplan-Meier survival curves of mice intracranially implanted with GSCs expressing shUSP13 or shNT control. Disrupting USP13 significantly increased survival of mice bearing GSC-derived xenografts. ***, $P < 0.001$; shNT versus shUSP13. Log-rank analysis was used to assess the significance. Five mice per group were used. (E) IB analysis of USP13 and c-Myc in GSCs (T387) transduced with the Tet-on–inducible shUSP13 (pTRIPZ-shUSP13) and treated with doxycycline (Dox) or vehicle control (Ctrl) for 3 d. Inducible knockdown of USP13 decreased c-Myc protein levels in GSCs. Mass is shown in kilodaltons. (F) Growth curves of GSCs (T387) transduced the inducible shUSP13 (pTRIPZ-shUSP13) and incubated with doxycycline or control. Then, cells were measured for cell growth over a time

sion levels were also much higher in human NPC lines with low c-Myc expression than those in GSC populations with high levels of c-Myc, as demonstrated by both IB analysis (Fig. 5 H) and immunofluorescence (Fig. 5 I). We confirmed that FBXL14 was expressed in differentiated cells ($GFAP^+$ and $TUJ1^+$) and NPCs ($SOX2^+$) in SVZs in adult and embryonic mouse brains (Fig. 5, J and K). Collectively, these data demonstrate that the ubiquitinase FBXL14 is preferentially expressed in the nonstem glioma cells and neural progenitors.

### Overexpression of FBXL14 promotes GSC differentiation and inhibits GBM tumor growth

As FBXL14 protein levels are much higher in NSTCs than in matched GSCs, we examined whether overexpression of FBXL14 in GSCs promoted cell differentiation and inhibited cell growth. We found that ectopic expression of FBXL14 (Flag-FBXL14) in GSCs not only accelerated the decrease of c-Myc protein levels, but also augmented the expression of differentiation markers (GFAP and MAP2) during a time course of serum-induced cell differentiation assay (Fig. 6 A). In addition, overexpression of FBXL14 accelerated c-Myc turnover in the presence of cycloheximide (not depicted), but treatment with the proteasome inhibitor MG132 rescued the c-Myc loss caused by FBXL14 overexpression (not depicted), indicating that FBXL14 plays a role in promoting c-Myc degradation to augment cell differentiation. Coimmunofluorescent staining of Flag-FBXL14 with the GSC marker (SOX2 or c-Myc) or the differentiation marker (GFAP or TUJ1) further validated that ectopic expression of FBXL14 in GSCs indeed promoted GSC differentiation (Fig. 6, B–E; and not depicted). The expression of FBXL14 also inhibited GSC tumorsphere formation (Fig. 6, F–I) and cell growth (Fig. 6 J). These data demonstrated that overexpression of FBXL14 in GSCs reduced c-Myc protein and promoted GSC differentiation to inhibit cell growth.

Given the effects of FBXL14 overexpression on inhibiting GSC growth in vitro, we then examined whether overexpression of FBXL14 impacted tumor propagating capacity of GSCs in vivo. GSCs transduced with luciferase and Flag-FBXL14 or vector control were transplanted into brains of immunocompromised mice and then monitored by bioluminescent imaging. Bioluminescent analysis demonstrated that FBXL14 overexpression significantly suppressed the tumor growth of GSCs in an intracranial xenograft mouse model (Fig. 7, A and B). Mice sacrificed at day 21 after GSC transplantation showed that mice bearing the GSCs expressing Flag-FBXL14 developed much smaller tumors than the control group (Fig. 7 C). As a consequence, the survival of mice bearing the FBXL14-overexpressing GSCs was significantly longer than that of the vector control group ($P < 0.001$; Fig. 7 D). IHC staining confirmed that forced expression of FBXL14 reduced c-Myc protein, decreased cell proliferation, and increased apoptosis in the xenograft tumors (not depicted). To further validate the tumor-suppressive role of FBXL14 in established tumors, we applied the Tet-on inducible overexpression system to examine the impact of FBXL14 expression on tumor growth in GSC-derived xenografts. An in vitro analysis showed that induced overexpression of FBXL14 decreased c-Myc protein and inhibited GSC proliferation (Fig. 7, E and F). In vivo bioluminescent analysis demonstrated that induced overexpression of FBXL14 by doxycycline treatment significantly suppressed intracranial tumor growth (Fig. 7, G and H). As a consequence, mice intracranially transplanted with GSCs overexpressing FBXL14 induced by doxycycline significantly extended their survival relative to the control group (Fig. 7 I). We conclude that FBXL14 exhibits tumor-suppressive capacity, and sustained expression of FBXL14 potently inhibits the tumorigenic capacity of GSCs in vivo.

### FBXL14 mediates c-Myc ubiquitination, whereas USP13 stabilizes c-Myc through deubiquitination

Because FBXL14 interacts with c-Myc and functions as a ubiquitin E3 ligase and overexpression of FBXL14 in GSCs rapidly reduced c-Myc protein levels, we speculated that FBXL14 might mediate c-Myc ubiquitination to promote protein degradation. A ubiquitination assay demonstrated that overexpression of FBXL14 markedly increased polyubiquitination of c-Myc (Fig. 8 A). In contrast, FBXL14 knockdown reduced c-Myc ubiquitination, leading to elevated c-Myc protein levels (Fig. 8 B). As threonine 58 (T58) and serine 62 (S62) residues on human c-Myc have been shown to be critical for the ubiquitin-mediated degradation of c-Myc protein (Yada et al., 2004; Hollern et al., 2013), we mutated the T58 or/and S62 to alanine (T58A or/and S62A) on c-Myc and then examined the effects of these mutations on protein stability. The ubiquitination assay indicated that both mutations (either alone or in combination) abolished the elevated

course (day 0 to day 8). Disrupting USP13 significantly inhibited the growth of GSCs. $n = 5$. **, $P < 0.01$; ***, $P < 0.001$. Student's $t$ test was used to assess the significance. Data are from three independent experiments. (G and H) In vivo bioluminescent imaging of GBM xenografts derived from luciferase-labeled GSCs expressing inducible shUSP13 and treated with doxycycline or vehicle control. GSCs (T387) were transduced with the Tet-on–inducible shUSP13 (pTRIPZ-shUSP13) and then transplanted into brains of immunocompromised mice ($10^4$ cells per animal). Mice bearing the intracranial xenografts were closely monitored. 7 d after GSC transplantation, mice were treated with the vehicle control or doxycycline (2 mg/ml in drinking water) to induce expression of shUSP13 in xenografts. (G) Representative images at the indicated days are shown. (H) Bioluminescent quantification at day 21 indicated that induced disruption of USP13 by doxycycline attenuated GSC tumor growth in mouse brains. $n = 5$. **, $P < 0.01$. Student's $t$ test was used to assess the significance. Five mice per group were used. (I) Kaplan-Meier survival curves of mice intracranially implanted with the GSCs (T387) transduced with the pTRIPZ-shUSP13 for 7 d and then treated with doxycycline or the vehicle control. Induced disruption of USP13 significantly increased the survival of mice bearing the GSC-derived xenografts. **, $P < 0.01$. Log-rank analysis was used. Five mice per group were used. Data are mean ± SD.

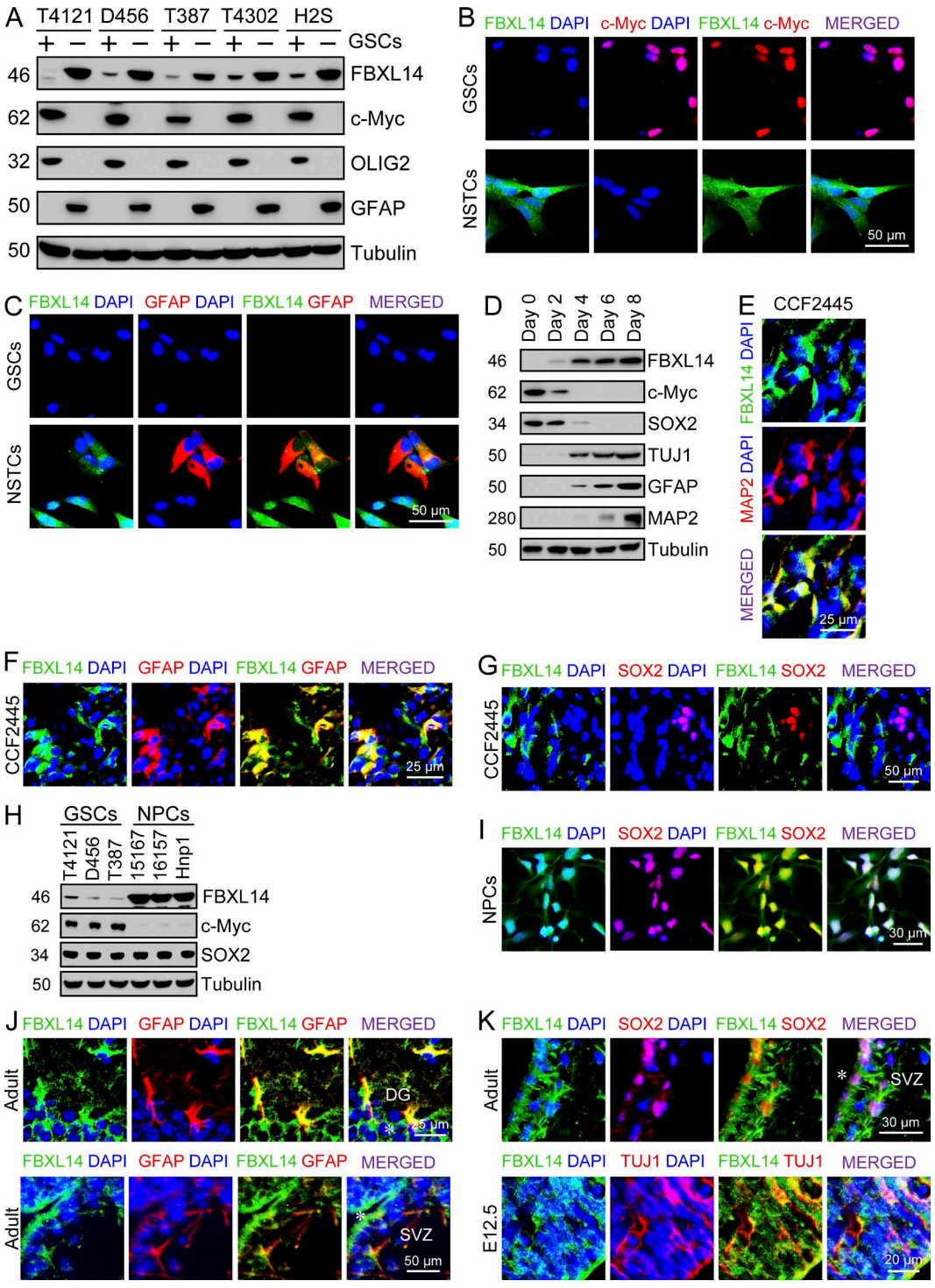


Figure 5. **FBXL14 is preferentially expressed in nonstem glioma cells and NPCs.** (A) IB analysis of FBXL14, c-Myc, OLIG2, and GFAP in GSCs (+) and matched NSTCs (–) isolated from five GBM tumors. OLIG2 and c-Myc are GSC markers, whereas GFAP is a marker for differentiated cells (astrocytes). FBXL14 is preferentially expressed in NSTCs. (B) Immunofluorescent staining of FBXL14 (green) and c-Myc (red) in GSCs and matched NSTCs derived from T387 xenografts. Nuclei were counterstained with DAPI (blue). FBXL14 is expressed in NSTCs but rarely expressed in the GSCs. (C) Immunofluorescent staining of FBXL14 (green) and the differentiation marker (GFAP; red) in GSCs and matched NSTCs derived from T387 xenografts. Nuclei were counterstained with DAPI (blue). FBXL14 is preferentially expressed in the NSTCs. (D) IB analysis of FBXL14, the GSC markers (c-Myc and SOX2), and the differentiated cell markers (GFAP, TUJ1, and MAP2) during serum-induced GSC differentiation. T4121 GSCs were cultured in DMEM containing 10% FBS to induce differentiation and harvested on the indicated days for immunoblotting. c-Myc and SOX2 gradually decreased, whereas FBXL14 along with the differentiation markers GFAP

c-Myc ubiquitination caused by FBXL14 overexpression (Fig. 8 C). In addition, the T58A mutant attenuated the ability of c-Myc to interact with FBXL14 (not depicted), thus suggesting that the T58 residue on human c-Myc is required for FBXL14-mediated ubiquitination. Collectively, these data demonstrated that FBXL14 functions as a ubiquitin E3 ligase to promote c-Myc ubiquitination and degradation and thus down-regulates c-Myc protein levels in glioma cells.

As USP13 functions as a deubiquitinase that also interacts with c-Myc (Fig. 1) and the preferential expression of USP13 in GSCs positively regulates c-Myc protein levels (Fig. 3, B and C), we hypothesized that USP13 might mediate deubiquitination of c-Myc protein to prevent its degradation and stabilize c-Myc in GSCs. To test this hypothesis, we examined whether USP13 knockdown impacted c-Myc polyubiquitination. The ubiquitination assay demonstrated that disruption of USP13 by shRNA markedly increased c-Myc ubiquitination and reduced c-Myc protein level in GSCs (Fig. 8 D). To validate this result, we examined the effect of USP13 overexpression on c-Myc ubiquitination. GSCs were transduced with wild-type USP13 (Flag-USP13) or the catalytically inactive mutant (USP13-C345A; Zhao et al., 2011) and then subjected to ubiquitination assay of c-Myc protein. Consistently, overexpression of the wild type but not the USP13 mutant reduced c-Myc ubiquitination and resulted in elevated c-Myc protein levels (Fig. 8 E). Interestingly, we found that the C345A-USP13 mutant played a dominant-negative role in c-Myc stabilization as overexpression of this catalytically inactive mutant reduced c-Myc protein levels and promoted expression of differentiation markers (not depicted). Collectively, these data demonstrate that USP13 stabilizes c-Myc protein through deubiquitination in GSCs.

### The antagonistic functions of USP13 and FBXL14 determine glioma cell fate through c-Myc regulation

Our data have demonstrated that USP13 mediates deubiquitination of c-Myc, whereas FBXL14 facilitates c-Myc ubiquitination in glioma cells. This suggests that USP13 and FBXL14 function as an opposing pair of deubiquitinase and ubiquitin E3 ligase to regulate c-Myc protein stability at the posttranslational level. To further validate this hypothesis, we reconstituted a regulatory system by overexpressing USP13 with FBXL14 or knocking down USP13 and FBXL14 to directly assess c-Myc regulation by USP13-mediated deubiquitination and FBXL14-mediated ubiquitination in glioma cells (GSCs or NSTCs). Overexpression of USP13 reduced c-Myc ubiquitination, and forced expression of FBXL14 increased c-Myc ubiquitination (Fig. 8 F). Importantly, overexpression of USP13 together with FBXL14 abolished the increased c-Myc ubiquitination caused by FBXL14 overexpression (Fig. 8 F, last lane). Moreover, USP13 knockdown increased c-Myc ubiquitination, whereas FBXL14 knockdown reduced c-Myc ubiquitination (Fig. 8 G). Silencing FBXL14 alongside USP13 disruption attenuated the increased c-Myc ubiquitination caused by USP13 disruption (Fig. 8 G). The regulation of c-Myc protein level by these two counterparts (USP13 and FBXL14) was further confirmed by coimmunofluorescent staining (not depicted). Functionally, overexpression of USP13 and FBXL14 together in GSCs abolished the enhanced cell differentiation induced by FBXL14 overexpression (not depicted), and knockdown of FBXL14 and USP13 together in GSCs attenuated the increased differentiation induced by USP13 disruption (not depicted). These data further confirmed that USP13-mediated deubiquitination and FBXL14-mediated ubiquitination serve opposite roles in the regulation of c-Myc protein levels as a control mechanism for cell fate determination of GSCs (stemness or differentiation).

### The ubiquitination-insensitive mutant T58A–c-Myc rescued the effects caused by USP13 disruption or FBXL14 overexpression

As USP13 and FBXL14 function as oppositional counterparts to regulate c-Myc protein levels in glioma cells, we further examined whether the ubiquitination-insensitive mutant T58A–c-Myc (Yada et al., 2004; Hollern et al., 2013) could rescue the phenotype caused by USP13 knockdown or FBXL14 overexpression in glioma cells in vitro and in vivo. As the T58A–c-Myc mutant attenuated its ability to interact with FBXL14 (not depicted), this mutant is resistant to FBXL14-mediated ubiquitination. The expression level of the exogenous c-Myc mutant (Flag-Myc-T58A) was adjusted to the similar level of endogenous c-Myc (Fig. 9, A and B). We confirmed that this c-Myc mutant is insensitive to ubiquitination-mediated degradation, as USP13 knockdown or FBXL14 overexpression did not affect the protein level of the mutant (T58A–c-Myc) but markedly reduced endogenous c-Myc in GSCs (Fig. 9, A and B). Ectopic expression of the ubiquitin-insensitive c-Myc mutant in GSCs rescued the

(for astrocytes) and MAP2 (for neurons) increased during GSC differentiation. (E–G) Immunofluorescent staining of FBXL14 and the differentiation marker MAP2 (E) or GFAP (F) or GSC marker SOX2 (G) in a primary GBM (CCF2445). Frozen sections of GBM were coimmunostained with specific antibodies against FBXL14 (green) and a differentiation marker (MAP2 or GFAP; red) or a GSC marker (SOX2; red) and then counterstained with DAPI to show nuclei. FBXL14 is coexpressed in the glioma cells expressing the differentiation markers but not the GSC marker. (H) IB analysis of FBXL14, c-Myc, and SOX2 in GSC populations and human NPC lines. GSCs expressed much less FBXL14 but much more c-Myc than NPCs. (I) Immunofluorescent staining of FBXL14 and SOX2 in human NPCs. NPCs were coimmunostained with specific antibodies against FBXL14 (green) and a stem cell marker (SOX2; red) and then counterstained with DAPI (blue). FBXL14 is expressed in NPCs. (J and K) Immunofluorescent staining of FBXL14 and GFAP, SOX2, or TUJ1 in the dentate gyrus (DG) or SVZ in the adult or embryonic mouse brain. Frozen sections of normal mouse brains were coimmunostained with specific antibodies against FBXL14 (green) and an NPC marker (SOX2; red), an astrocyte marker (GFAP; red), or a neuronal marker (TUJ1; red) and then counterstained with DAPI (blue) to show nuclei. Asterisks indicate the dentate gyrus (J, top) or the SVZ (J, bottom; and K). (A, D, and H) Mass is shown in kilodaltons.

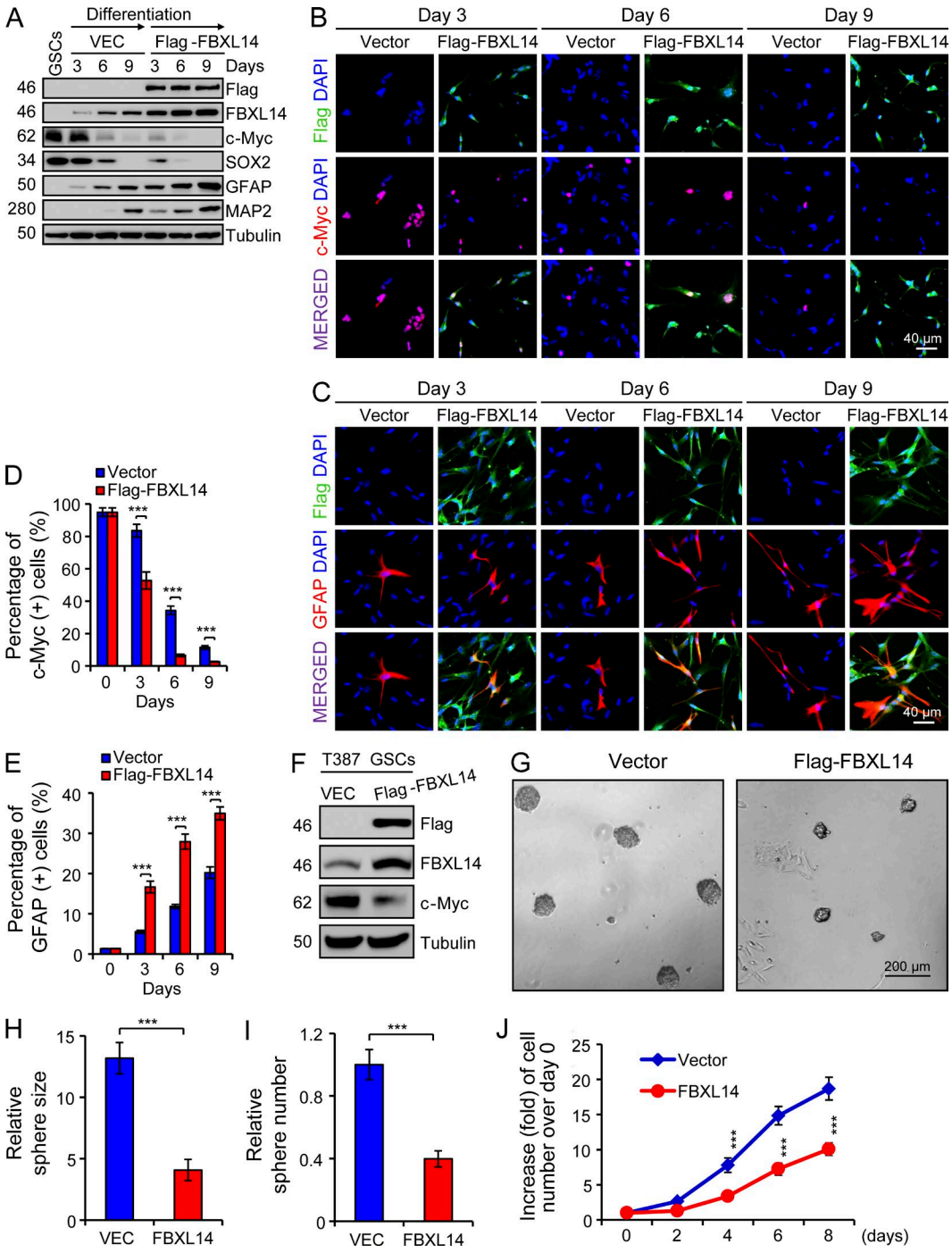


Figure 6. **Overexpression of FBXL14 promoted GSC differentiation and inhibited GSC tumor growth.** (A) IB analysis of FBXL14, c-Myc, SOX2, GFAP, and MAP2 in the GSCs transduced with Flag-FBXL14 expression through lentiviral infection during a time course of differentiation. Forced expression of FBXL14 in GSCs accelerated expression of differentiated cell markers (GFAP and MAP2) and augmented loss of GSC markers (c-Myc and SOX2) during serum-induced GSC differentiation. VEC, vector. (B–E) Immunofluorescent staining of Flag-FBXL14 and c-Myc (B) or GFAP (C) in GSCs (T387) expressing Flag-FBXL14 or vector control during a time course of GSC differentiation induced by serum (FBS). Cells were counterstained with DAPI (blue) to mark nuclei. Quantifications show that forced expression of FBXL14 significantly accelerated the reduction of c-Myc–positive cells (D) and increased percentage of GFAP-positive cells (E) during serum-induced GSC differentiation. $n = 4$. Data are from three independent experiments, and representative images are shown. (F–I) The effect of FBXL14 overexpression on GSC tumorsphere formation. GSCs (T387) were transduced with Flag-FBXL14 or vector control. (G) Ectopic expression of Flag-FBXL14 reduced tumorsphere formation of GSCs. (H and I) Quantifications show that forced expression of FBXL14 significantly decreased GSC tumorsphere size (H) and number (I). $n = 3$–4. Data are from three independent experiments, and representative images are shown.

impaired tumorsphere formation caused by USP13 knockdown or FBXL14 overexpression (Fig. 9, C–H) and restored the cell growth impaired by USP13 disruption or FBXL14 overexpression (not depicted). Immunofluorescent analysis indicated that ectopic expression of the mutant c-Myc in GSCs reduced the differentiation induced by FBXL14 overexpression (not depicted). Importantly, an orthotopic tumor formation assay demonstrated that ectopic expression of the ubiquitin-insensitive c-Myc mutant (T58A–c-Myc) restored GSC tumor growth which was attenuated by USP13 down-regulation or FBXL14 up-regulation (Fig. 9, I–L). Furthermore, ectopic expression of the mutant c-Myc abolished the increased survival of mice bearing GSC-derived xenografts expressing shUSP13 or Flag-FBXL14 (Fig. 9, M and N). In addition, terminal deoxynucleotidyl transferase deoxyuridine triphosphate nick-end labeling (TUNEL) assay demonstrated that expression of the mutant c-Myc diminished the increased apoptosis caused by USP13 disruption in GSC-derived xenografts (not depicted). Immunofluorescence analysis confirmed that ectopic expression of the mutant c-Myc reduced the cell differentiation (measured by $GFAP^+$ cells) induced by FBXL14 overexpression in GSC-derived xenografts (not depicted) and restored cell proliferation inhibited by FBXL14 overexpression as measured by Ki-67 staining (not depicted). Collectively, these data demonstrate that the ubiquitination-insensitive mutant of c-Myc is able to rescue the phenotypes caused by USP13 knockdown or FBXL14 overexpression in vitro and in vivo, which supports that USP13 and FBXL14 mediate posttranslational regulation of c-Myc to control the stem cell–like phenotype and tumorigenic potential of GSCs.

### USP13 expression showed an inverse correlation with the survival of GBM patients, but FBXL14 displayed a positive correlation

To confirm the clinical relevance of preferential expression of USP13 in GSCs and FBXL14 in NSTCs, we analyzed the potential correlation of USP13 and FBXL14 expression with the prognosis of GBM patients in the Rembrandt database. Kaplan-Meier survival curves demonstrated a significant inverse correlation between USP13 expression and the overall survival of GBM patients (Fig. 10 A). Higher expression of USP13 in GBMs predicts worse survival of the patients. In contrast, FBXL14 expression is positively correlated with the overall survival of GBM patients (Fig. 10 B). Higher FBXL14 expression informed better patient survival. In addition, a correlation analysis between USP13 or FBXL14 and the GSC marker (SOX2 or OLIG2) in the dataset confirmed that USP13 expression was positively correlated with the expression of SOX2 and OLIG2 (Fig. 10 C), whereas the expression of FBXL14 is negatively correlated with expression of SOX2 and OLIG2 (Fig. 10 D). Furthermore, analysis of the Rembrandt database demonstrated that USP13 expression was significantly increased in high-grade gliomas relative to low-grade gliomas and normal human brain tissues (Fig. 10 E), whereas FBXL14 expression was significantly decreased in high-grade gliomas (Fig. 10 F). Collectively, these data demonstrate that USP13 and FBXL14 expression may serve as prognostic markers for GBM.

## DISCUSSION

GBMs are highly lethal brain tumors and are resistant to current treatments (Stupp et al., 2005; Wen and Kesari, 2008). The presence of self-renewing and tumorigenic GSC populations in GBM tumors contributes to therapeutic resistance and treatment failure (Bao et al., 2006a; Liu et al., 2006; Chen et al., 2012). Thus, eliminating GSCs or impairing their growth through GSC differentiation may effectively improve GBM treatment. GSCs are maintained by a set of core SCTFs, including c-Myc (Wang et al., 2008; Gargiulo et al., 2013; Annibali et al., 2014; Kozono et al., 2015). Several studies have demonstrated that c-Myc oncoprotein plays crucial roles in maintaining the self-renewal, proliferation, and tumorigenic potential of cancer stem cells including GSCs (Wang et al., 2008; David et al., 2010; Rahl et al., 2010; Saborowski et al., 2014; Terunuma et al., 2014). Cellular c-Myc protein levels are tightly regulated by both transcriptional control and posttranslational regulation. Although the posttranslational modification of c-Myc has been studied in leukemia stem cells (King et al., 2013), the regulatory control of c-Myc by the ubiquitination and deubiquitination system in GSCs has not been elucidated. In this study, we demonstrated that USP13-mediated deubiquitination and FBXL14-mediated ubiquitination regulate c-Myc protein levels in glioma cells and play a critical role in controlling the maintenance or differentiation of GSCs (Fig. 10 G). USP13 stabilizes c-Myc through deubiquitination to promote GSC self-renewal, proliferation, and tumor formation. In contrast, the ubiquitin E3 ligase FBXL14 mediates c-Myc ubiquitination and subsequent degradation to induce GSC differentiation and inhibit GSC tumor growth. USP13 and FBXL14 function as antagonizing counterparts to regulate c-Myc protein levels and control cell fate determination, as well as the tumorigenic potential of glioma cells. We have demonstrated that disruption of USP13 or forced expression of FBXL14 potently suppressed GSC tumor growth in GBM xenograft models, suggesting that manipulating the posttranslational regulation of c-Myc in GSCs by targeting its deubiquitinase USP13 may effectively control GBM tumor progression and potentially overcome GSC-mediated therapeutic resistance.

(J) Growth curves of GSCs expressing Flag-FBXL14 or vector control. GSCs (T387) were transduced with Flag-FBXL14 or vector control through lentiviral infection and then measured for cell growth over a time course. Ectopic expression of FBXL14 significantly inhibited GSC growth. $n = 4$. Data are from three independent experiments. Data are mean ± SD. ***, $P < 0.001$. Student's *t* test was used to assess the significance. (A and F) Mass is shown in kilodaltons.

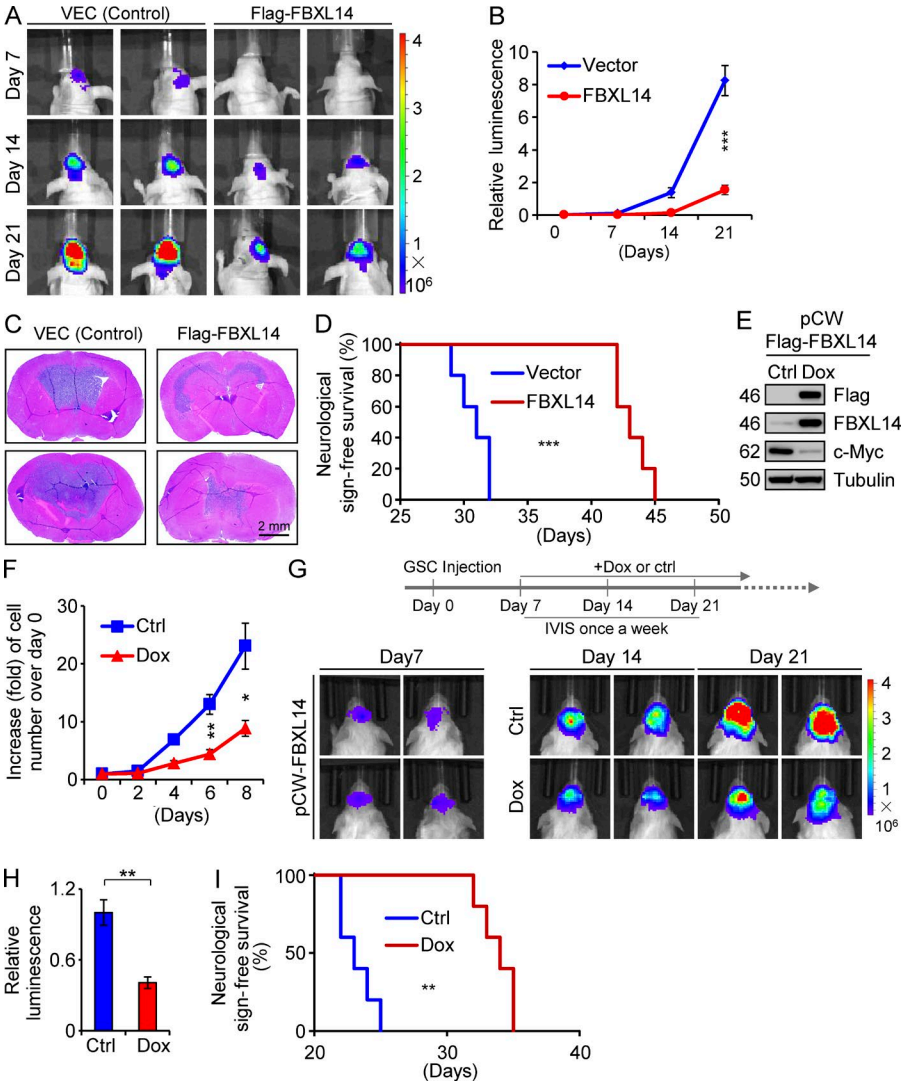


Figure 7. **Overexpression of FBXL14 inhibited GBM tumor growth and promoted animal survival.** (A and B) In vivo bioluminescent imaging of GBM xenografts derived from luciferase-expressing GSCs transduced with FBXL14 or vector (VEC) control. GSCs (T387) were transduced with luciferase and Flag-FBXL14 or vector control and then transplanted into brains of immunocompromised mice ($5 \times 10^3$ cells per animal). Mice bearing the intracranial xenografts were monitored after GSC transplantation. (A) Representative images at the indicated days are shown. (B) Luminescence quantification indicated that ectopic expression of FBXL14 significantly attenuated GSC tumor growth in mouse brains. Data are mean ± SD. $n = 5$. ***, $P < 0.001$. Student's $t$ test was used to assess the significance. Five mice per group were used. (C) Representative images of mouse brain sections from mice intracranially implanted with the GSCs transduced with Flag-FBXL14 or vector control. GSCs (T387) were transduced with Flag-FBXL14 or vector control through lentiviral infection for 48 h and then transplanted into mouse brains. Cross sections (hematoxylin and eosin stained) of the mouse brains harvested on day 21 after injection are shown. (D) Kaplan-Meier survival curves of mice intracranially implanted with the GSCs expressing Flag-FBXL14 or vector control. Ectopic expression of FBXL14 significantly increased survival of mice bearing the GSC-derived xenografts. Log-rank analysis was used. Five mice per group were used. (E) IB analysis of FBXL14 and c-Myc in GSCs (T387) transduced with inducible FBXL14 (pCW-Flag-FBXL14) and then treated with doxycycline (Dox) for 3 d. FBXL14 overexpression decreased c-Myc protein levels. Mass is shown in kilodaltons. Ctrl, control. (F) Growth curves of GSCs transduced with inducible FBXL14 expression and treated with doxycycline or control. Cells were measured for cell growth over a time course (day 0 to day 8). Overexpression of FBXL14 significantly inhibited the growth of GSCs. Data are mean ± SD. $n = 3$. Student's $t$ test was used to assess the significance. Data are from three independent experiments. (G and H) In vivo bioluminescent imaging of GBM xenografts derived from the luciferase-labeled GSCs transduced with inducible FBXL14 overexpression and treated with doxycycline or control. GSCs (T387) were transduced with inducible FBXL14 expression (pCW-Flag-FBXL14) and then transplanted into brains of immunocompromised mice ($10^4$ cells per animal). Mice bearing the intracranial xenografts were closely monitored. 7 d after GSC transplantation, mice were treated with 2 mg/ml doxycycline in drinking water to induce expression of FBXL14 in xenografts. (G) Representative images at the indicated days are shown. (H) Bioluminescence quantification indicated that induced overexpression of FBXL14 attenuated GSC tumor growth in mouse brains at day 21. Data are mean ± SD. $n = 5$. Student's $t$ test was used to assess the significance. Five mice per group were used. (I) Kaplan-Meier survival curves of mice intracranially implanted with the GSCs transduced with pCW-Flag-FBXL14 for 7 d and then treated with doxycycline or control. Induced expression of FBXL14 significantly increased survival of mice bearing the GSC-derived xenografts. Log-rank analysis was used. Five mice per group were used. *, $P < 0.05$; **, $P < 0.01$; ***, $P < 0.001$.

c-Myc is a critical pleiotropic transcription factor regulating the expressions of many genes that control cell proliferation, growth, apoptosis, metabolism, ribosomal biogenesis, and the maintenance of stem cells including cancer stem cells (Gordan et al., 2007a,b; Nieminen et al., 2007; Wang et al., 2008; Gao et al., 2009; Rahl et al., 2010; Nie et al., 2012; Masui et al., 2013). The maintenance of c-Myc protein level and activity is crucial for normal cell proliferation and growth during homoeostasis. Increased c-Myc levels or its activity through aberrant overexpression or dysregulated posttranslational modification is closely associated with tumorigenesis and malignant progression of many human cancers (Cole and Cowling, 2008; Pan et al., 2015; Sun et al., 2015). The oncogenic role of the *c-Myc* gene has been shown in various

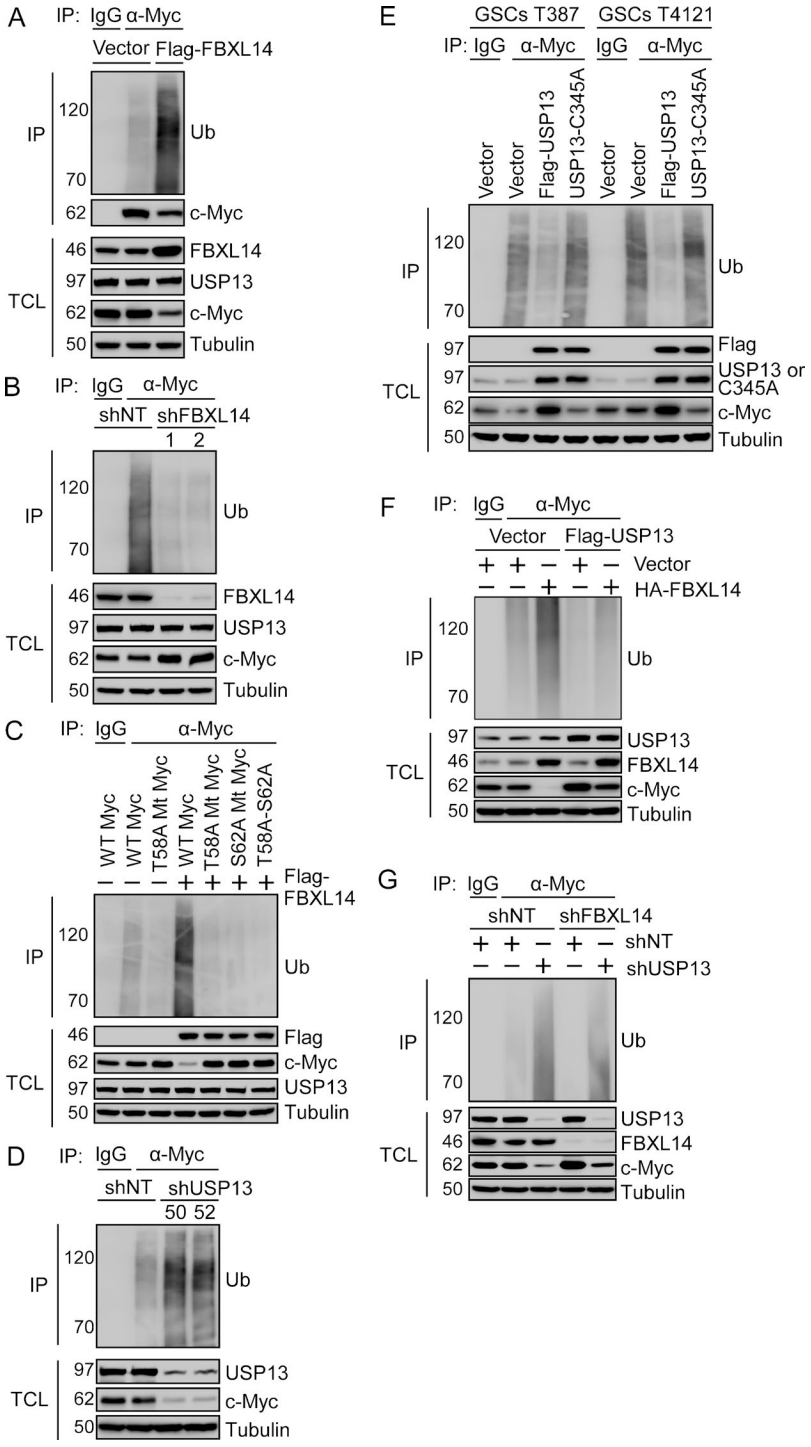


Figure 8. **FBXL14 mediates ubiquitination and degradation of c-Myc, whereas USP13 stabilizes c-Myc protein through deubiquitination.** (A) Ubiquitination (Ub) assay showing that overexpression of FBXL14 promoted degradation of c-Myc in GSCs. GSCs (T387) were transduced with Flag-FBXL14 or vector control through lentiviral infection for 48 h, treated with the proteasome inhibitor MG132 for 6 h, harvested for IP of c-Myc with an anti–c-Myc antibody, and then immunoblotted with anti-ubiquitin antibody. Total cell lysates (TCL) were also immunoblotted with antibodies against FBXL14, USP13, c-Myc, and tubulin. (B) Ubiquitination assay showing that FBXL14 knockdown decreased c-Myc ubiquitination in GSCs. GSCs (T387) were transduced with shFBXL14 or shNT through lentiviral infection for 48 h and then treated with the proteasome inhibitor MG132 for 6 h before collecting samples. Cell lysates were immunoprecipitated with an anti–c-Myc antibody and then immunoblotted with anti-ubiquitin antibody. (C) Ubiquitination assay showing that FBXL14 mediated ubiquitination of wild-type c-Myc (lane 4) but not the ubiquitin-insensitive c-Myc mutants (Mt): T58A-Myc (lane 5), S62A-Myc (lane 6), and T58A-S62A-Myc (lane 7). Flag-FBXL14 or vector control and wild-type c-Myc or the c-Myc mutant were overexpressed in 293FT cells and then subjected to ubiquitination assay and IB analysis. (D) Ubiquitination assay showing that USP13 knockdown increased c-Myc ubiquitination and decreased c-Myc protein levels in GSCs. GSCs (T387) were transduced with shUSP13 (shUSP13-50 or shUSP13-52) or shNT control for 48 h and then treated with the proteasome inhibitor MG132 for 6 h before collecting samples. Cell lysates were immunoprecipitated with an anti–c-Myc antibody and then immunoblotted with anti-ubiquitin antibody. (E) Ubiquitination assay showing that c-Myc ubiquitination was specifically attenuated by wild-type USP13 but not catalytic dead mutant USP13 (C345A). GSCs (T387 or T4121) were transduced with Flag-USP13, Flag-USP13-C345A, or vector control for 48 h, treated with the proteasome inhibitor MG132 for 6 h, and then subjected to analysis of c-Myc ubiquitination and IB analyses. (F) Ubiquitination analysis showing that USP13-mediated deubiquitination antagonizes FBXL14-mediated c-Myc ubiquitination to regulate c-Myc protein levels in GSCs. GSCs (T387) were transduced with HA-FBXL14, Flag-USP13, Flag-USP13 plus HA-FBXL14, or vector control for 2 d through lentiviral infection, treated with MG132 for 6 h, and harvested for ubiquitination assay of c-Myc and IB analyses. FBXL14 overexpression alone increased c-Myc ubiquitination (lane 3), whereas USP13 overexpression alone decreased c-Myc ubiquitination (lane 4). However, USP13 and FBXL14 double overexpression attenuated the increased c-Myc ubiquitination induced by FBXL14 overexpression (lane 5). (G) Ubiquitination assay showing that c-Myc protein level was regulated by USP13-mediated deubiquitination and FBXL14-induced ubiquitination in GSCs. GSCs (T387) were differentiated for 2 d and transduced with shUSP13, shFBXL14, shUSP13 plus shFBXL14, or shNT for 2 d through lentiviral infection, treated with MG132 for 6 h, and then collected for ubiquitination analysis and IB analyses. USP13 knockdown alone increased c-Myc ubiquitination (lane 3), whereas FBXL14 knockdown alone decreased c-Myc ubiquitination (lane 4). However, USP13 and FBXL14 double knockdown attenuated the increased c-Myc ubiquitination induced by USP13 knockdown (lane 5). Mass is shown in kilodaltons.

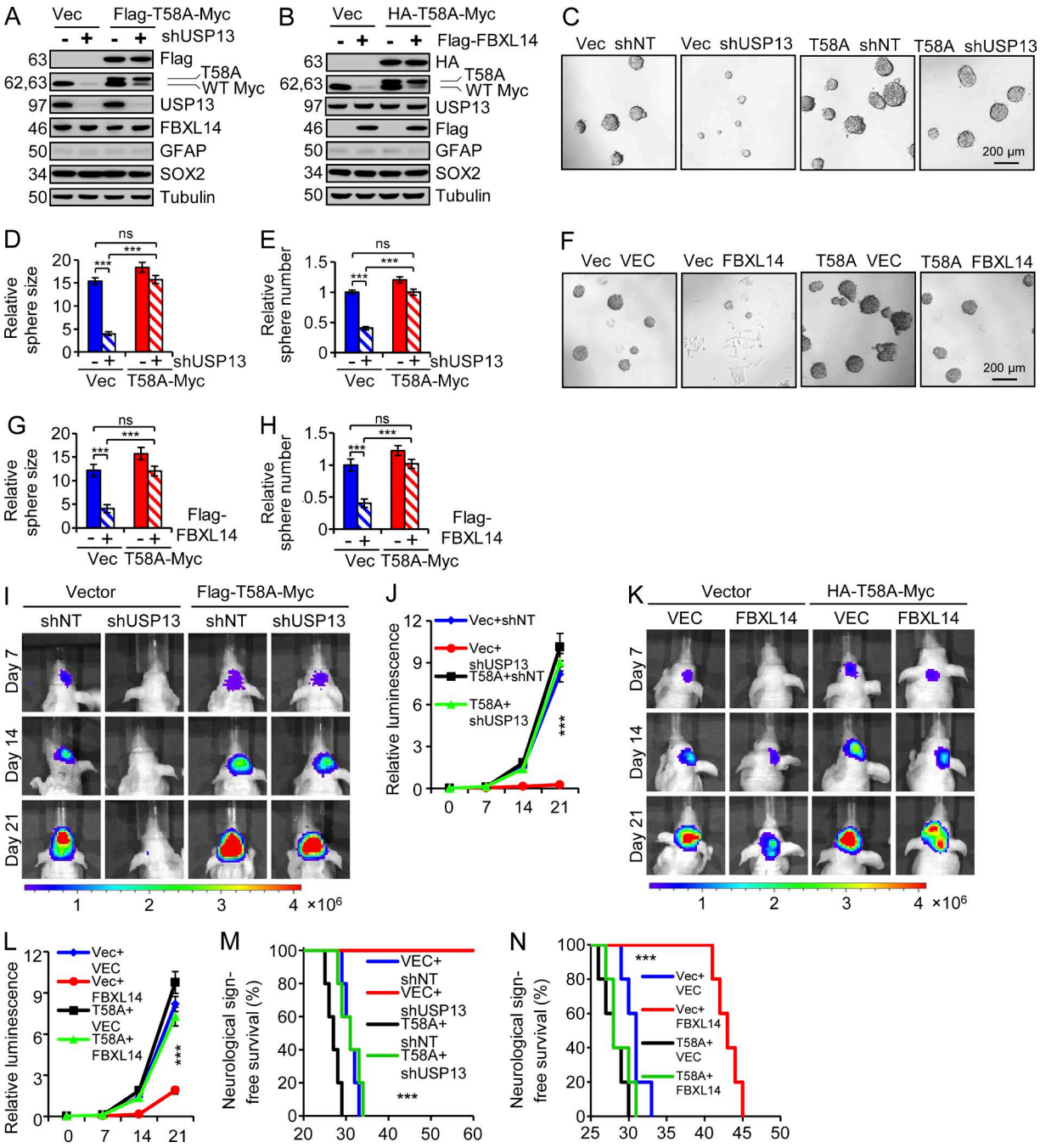


Figure 9. **T58A–c-Myc mutant rescued the phenotype caused by USP13 knockdown or FBXL14 overexpression.** (A) IB analysis of Flag-T58A–c-Myc mutant, endogenous c-Myc (WT), USP13, FBXL14, GFAP, and SOX2 in the T387 GSCs transduced with Flag-T58A–c-Myc or vector (Vec) control in combination with shUSP13 or shNT control. USP13 knockdown decreased the endogenous wild-type c-Myc but not the ectopic Flag-T58A–c-Myc mutant. (B) IB analysis of Flag-FBXL14, HA-T58A–c-Myc mutant, endogenous c-Myc (WT), USP13, GFAP, and SOX2 in the GSCs transduced with HA-T58A–c-Myc or vector control in combination with Flag-FBXL14 or vector control. Ectopic expression of FBXL14 decreased endogenous wild-type c-Myc but not the HA-T58A–c-Myc mutant. (A and B) Mass is shown in kilodaltons. (C–E) Tumorsphere formation of GSCs transduced with Flag-T58A–c-Myc or vector control in combination with shUSP13 or shNT control. (C) Representative images (phase contrast) of tumorspheres are shown. Ectopic expression of Flag-T58A–c-Myc mutant in GSCs rescued the impaired tumorsphere formation caused by USP13 disruption. (D and E) Quantification indicated that ectopic expression of the T58A–c-Myc mutant in GSCs rescued the decreased tumorsphere size (D) and number (E) caused by USP13 disruption. Data are mean ± SD. $n = 4$. ***, $P < 0.001$. Student's $t$ test was used to assess the significance. Data are from three independent experiments. (F–H) Tumorsphere formation of GSCs transduced with HA-T58A–c-Myc or vector control in combination with Flag-FBXL14 or vector (VEC) control. (F) Representative images (phase contrast) of tumorspheres are shown. Ectopic expression of the T58A–c-Myc mutant in GSCs rescued the reduced tumorsphere formation caused by FBXL14 overexpression.

tissues in mouse models (Lewis et al., 2003; Wang et al., 2011; Kim et al., 2012; Hollern et al., 2013). c-Myc protein level is tightly controlled by posttranslational modifications such as ubiquitin-mediated proteasomal degradation and deubiquitination. c-Myc protein is very unstable in nontransformed cells and is degraded by the ubiquitin–proteasome system (von der Lehr et al., 2003). Several ubiquitin E3 ligases including Fbw7, Skp2, and HectH9 have been shown to regulate c-Myc protein stability and activity (von der Lehr et al., 2003; Welcker et al., 2004; Adhikary et al., 2005). Similar to other posttranslational modifications, ubiquitination of c-Myc can be reversed by deubiquitination mediated by the ubiquitin-specific proteases. USP28, USP37, and USP36 have been shown to deubiquitinate and stabilize c-Myc protein in colon cells (Popov et al., 2007; Pan et al., 2015; Sun et al., 2015). These studies suggested that the ubiquitination and deubiquitination regulation of c-Myc by different pairs of ubiquitin E3 ligase and deubiquitinase may depend on cell context. Our study demonstrates that USP13 and FBXL14 are the main pair of deubiquitinases and ubiquitin E3 ligases that regulate c-Myc protein levels in glioma cells, which supports a cell type–specific posttranslational regulation of c-Myc.

In nontransformed cells, c-Myc protein is transiently stabilized upon stimulation of cell growth and is then quickly degraded by the ubiquitin-proteasome. The growth-regulated turnover of c-Myc usually involves two conserved phosphorylation sites (T58 and S62) within Myc box I (Welcker et al., 2004; Yada et al., 2004; Hollern et al., 2013). The phosphorylation of c-Myc at S62 in response to growth signals increases c-Myc protein stability, whereas T58 phosphorylation destabilizes c-Myc by facilitating S62 dephosphorylation and recruiting the ubiquitin E3 ligase to mediate c-Myc ubiquitination and degradation (Sears et al., 2000; Yeh et al., 2004; Hollern et al., 2013). Thus, T58 phosphorylation is required for ubiquitination-mediated c-Myc degradation. T58 mutations that prevent its phosphorylation and ubiquitination-mediated c-Myc degradation were found in a subset of Burkitt's lymphomas (Bhatia et al., 1993). Consistently, our data showed that the T58A–c-Myc mutant was insensitive to FBXL14-mediated ubiquitination and was able to rescue the phenotypes caused by FBXL14 overexpression. Importantly, we demonstrated that USP13, which functions as the deubiquitinase of c-Myc, was preferentially expressed in GSCs. USP13 stabilizes c-Myc to maintain the stem cell–like phenotype and tumorigenic potential of GSCs. As other known c-Myc deubiquitinases such as USP28, USP37, and USP36 are rarely expressed in glioma cells (not depicted), USP13 is likely to be the main deubiquitinase that maintains high levels of c-Myc for sustaining the stemness and tumorigenic capacity of GSCs.

USP13 has been proposed to mediate deubiquitination of the ubiquitinated proteins and thus reverses their degradation in cells (Zhao et al., 2011). Although USP13 is an orthologue of the well-characterized deubiquitinase USP5, it has been demonstrated that USP13 is very different from USP5, both in substrate preference and catalytic efficiency (Zhang et al., 2011). USP5 generally functions as a deubiquitinating enzyme for trimming unanchored polyubiquitin chains to maintain the homoeostasis of the free ubiquitin pool (Zhang et al., 2011), whereas USP13 lacks the ability to hydrolyze free polyubiquitin chain to monoubiquitin efficiently and does not act as a regulator for the free ubiquitin pool (Zhang et al., 2011). However, USP13 plays important roles in the regulation of specific protein substrates. Recent studies indicated that USP13 can deubiquitinate and regulate protein levels of Beclin-1, microphathalmia-associated transcription factor, Siah2, phosphatase

(G and H) Quantification indicated that ectopic expression of the T58A–c-Myc mutant in GSCs rescued the decreased tumorsphere size (G) and number (H) caused by FBXL14 overexpression. Data are mean ± SD. $n = 4$. ***, $P < 0.001$. Student's $t$ test was used to assess the significance. Data are from three independent experiments. (I and J) In vivo bioluminescent imaging of GBM xenografts derived from the luciferase-labeled GSCs transduced with Flag-T58A–c-Myc mutant or vector control in combination with shUSP13 or shNT control. The luciferase-labeled GSCs (T387) were transduced with Flag-T58A–c-Myc or vector control and shUSP13 or shNT through lentiviral infection and then transplanted into the brains of immunocompromised mice ($5 \times 10^3$ cells per animal). Mice bearing the intracranial xenografts were monitored after GSC transplantation. (I) Representative images at the indicated days are shown. (J) Quantification of luminescence indicates that ectopic expression of the T58A–c-Myc mutant restored the GSC tumorigenic potential impaired by USP13 disruption. Data are mean ± SD. $n = 5$. ***, $P < 0.001$; VEC + shUSP13 versus other groups. Student's $t$ test was used to assess the significance. Five mice per group were used. (K and L) In vivo bioluminescent imaging of GBM xenografts derived from luciferase-expressing GSCs transduced with HA-T58A–c-Myc mutant or vector control in combination with Flag-FBXL14 or vector control. GSCs (T387) were transduced with HA-T58A–c-Myc or vector control in combination with Flag-FBXL14 or vector control through lentiviral infection and then transplanted into immunocompromised mouse brains ($5 \times 10^3$ cells per animal). Mice bearing the intracranial xenografts were monitored after GSC transplantation. (K) Representative images at the indicated days are shown. (L) Luminescence quantification shows that ectopic expression of the c-Myc–T58A mutant restored GSC tumorigenic potential attenuated by ectopic expression of FBXL14. Data are mean ± SD. $n = 5$. ***, $P < 0.001$; VEC + FBXL14 versus other groups. Student's $t$ test was used to assess the significance. Five mice per group were used. (M) Kaplan-Meier survival curves of mice implanted with GSCs transduced with Flag-T58A–c-Myc or vector control in combination with shUSP13 or shNT control. Mice implanted with the GSCs were maintained until the development of neurological signs or for 60 d. Ectopic expression of the T58A–c-Myc mutant in GSCs significantly attenuated the increased survival of mice caused by USP13 disruption in the GSC-derived tumors. ***, $P < 0.001$; VEC + shUSP13 versus other groups. Log-rank analysis was used. Five mice per group were used. (N) Kaplan-Meier survival curves of mice implanted with GSCs transduced with HA-T58A–c-Myc or vector control in combination with Flag-FBXL14 or vector control. Mice implanted with the GSCs were maintained until the development of neurological signs or for 60 d. Ectopic expression of the T58A–c-Myc mutant in GSCs significantly attenuated the increased survival of mice caused by FBXL14 expression in the GSC-derived tumors. ***, $P < 0.001$; VEC + FBXL14 versus other groups. Log-rank analysis was used. Five mice per group were used.

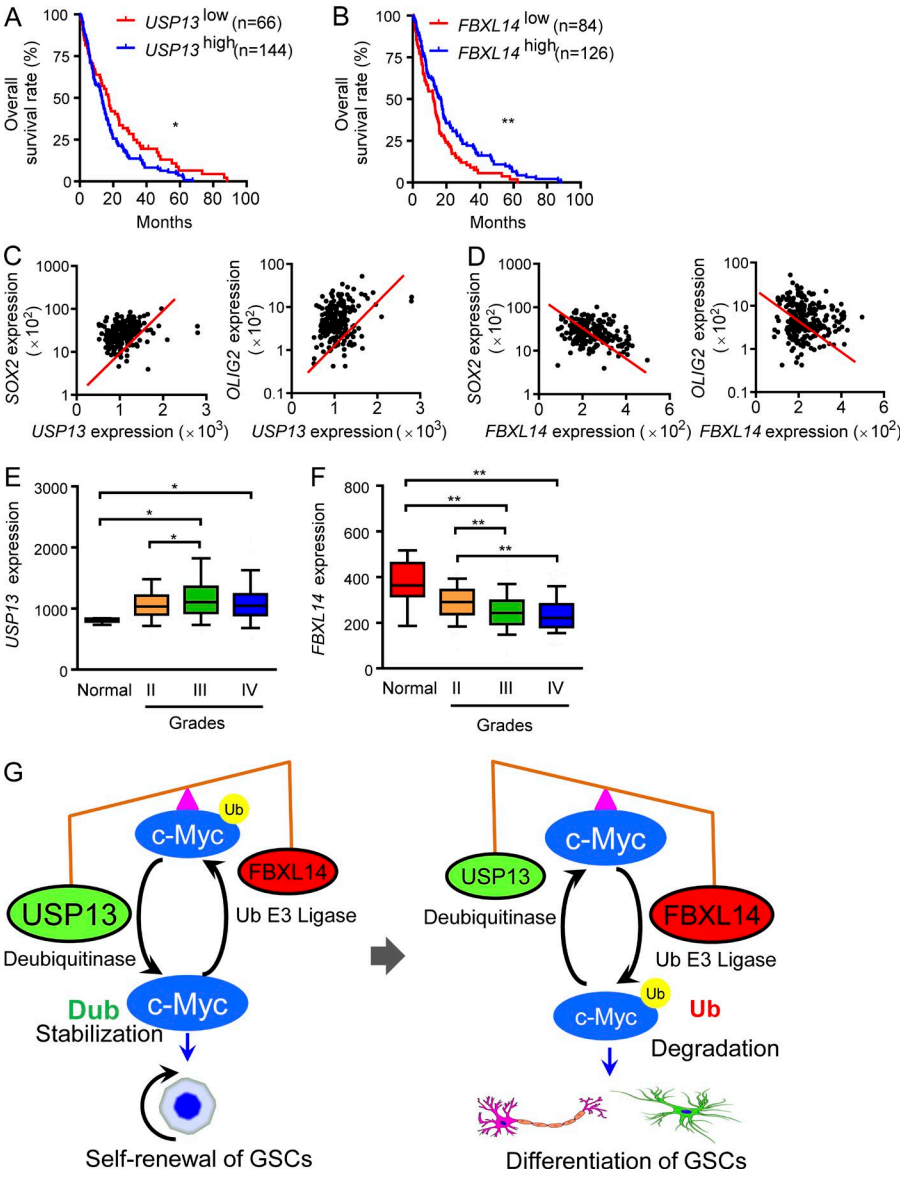


Figure 10. **USP13 and FBXL14 expressions are clinically associated with GBM patient survival, GSC makers, and glioma grades.** (A) Analysis of the Rembrandt database shows a significant inverse correlation between USP13 expression and the overall survival of GBM patients. Log-rank analysis was used. $n$ = 210. (B) Analysis of the Rembrandt database indicates a significant positive correlation between FBXL14 expression and the overall survival of GBM patients. Log-rank analysis was used. $n$ = 210. (C) Linear regression analysis of the Rembrandt database showed a significant positive correlation between USP13 expression and the expression of GSC markers SOX2 (R = 0.2493; P = 0.0002) or OLIG2 (R = 0.3363; P < 0.0001). Pearson's R correlation test was used. $n$ = 220. (D) Linear regression analysis of the Rembrandt database indicated a significant negative correlation between expression of FBXL14 and the expression of GSC markers SOX2 (R = −0.2912; P = 0.0002) or OLIG2 (R = −0.1600; P = 0.0175). Pearson's R correlation test was used. $n$ = 220. (E) Analysis of the Rembrandt database shows that USP13 expression was significantly higher in gliomas than that in normal brains. (F) Analysis of the Rembrandt database indicates that FBXL14 expression was lower in high-grade gliomas (III and IV) than in low-grade glioma (II) and normal brains. (E and F) Tukey's multiple comparisons test was used. Normal, $n$ = 7; grade II, $n$ = 99; grade III, $n$ = 85; grade IV, $n$ = 220. (G) A schematic illustration for the posttranslational regulation of c-Myc by USP13-mediated deubiquitination (Dub) and FBXL14-mediated ubiquitination (Ub) to determine the cell fate of glioma cells. The net balance between the FBXL14-mediated ubiquitination and the USP13-mediated deubiquitination controls c-Myc protein levels to determine the maintenance or differentiation of GSCs. *, P < 0.05; **, P < 0.01.

and tensin homolog, and STAT-1 (Liu et al., 2011; Scortegagna et al., 2011; Zhao et al., 2011; Yeh et al., 2013; Zhang et al., 2013), and the deubiquitination process of USP13 could also be orchestrated by Beclin-1 (Liu et al., 2011). USP13 also interacts with USP10, and the interaction increases USP13 deubiquitinating activity (Liu et al., 2011). In addition, USP13 interacts with the P97/valosin-containing protein complex, a key chaperone in ER-associated degradation (Chen et al., 2011), which increases the protein level of CD3δ, an ER-associated degradation substrate (Zhang et al., 2011). Interestingly, USP13 can antagonize gp78 (a ubiquitin E3 ligase) to deubiquitinate Ubl4A, a key component of the Bag6 chaperone complex in ER-associated degradation (Liu et al., 2014). Aberrant expression of USP13 has been associated with human cancers. It has been shown that the mRNA level of USP13 is elevated in thyroid tumors (Fontaine et al., 2009). Increased USP13 expression was also detected in melanomas, with a positive correlation with its substrate Siah2, suggesting its oncogenic role (Scortegagna et al., 2011). Our data demonstrate that USP13 plays an oncogenic role to maintain stemness and tumorigenic potential of GSCs in GBMs by stabilization of the c-Myc protein through deubiquitination. Importantly, USP13 expression is negatively correlated with the overall survival of GBM patients. Because USP13 is a deubiquitinating enzyme and is preferentially expressed in GSCs but rarely expressed in NPCs and targeting USP13 potently inhibits tumor growth, USP13 represents an attractive molecular target with a high therapeutic index for developing novel anti-GSC–specific therapeutics.

In contrast to the deubiquitinating role of USP13 in stabilizing c-Myc protein in GSCs, FBXL14 functions as a

ubiquitin E3 ligase and mediates c-Myc ubiquitination to promote c-Myc degradation in nonstem glioma cells (NSTCs). FBXL14 also regulates Snail2 protein during neural crest development in *Xenopus laevis* (Lander et al., 2011) and modulates ubiquitination and protein levels of mitogen-activated protein kinase phosphatase 3 (Mkp3) to regulate vertebrate axis formation in zebrafish (Zheng et al., 2012). In mammalian cells, FBXL14 has been demonstrated to target Snail1 for proteasome-mediated degradation through polyubiquitination (Viñas-Castells et al., 2010). Interestingly, FBXL14 expression was significantly down-regulated during hypoxia, a condition causing an increase of Snail1 protein but not its mRNA (Viñas-Castells et al., 2010). A decrease of FBXL14 expression was detected in tumors with high expression of Twist1 and carbonic anhydrase 9, two proteins up-regulated by hypoxia (Viñas-Castells et al., 2010). Our previous study showed that hypoxia promotes the maintenance of GSCs, and hypoxia may facilitate the dedifferentiation of nonstem glioma cells to GSCs (Li et al., 2009; Heddleston et al., 2010). However, the molecular mechanisms underlying the hypoxia-mediated maintenance of GSCs are not fully understood. As FBXL14 is highly expressed in NSTCs and low expressed in GSCs and FBXL14 functions as a ubiquitin E3 ligase to promote c-Myc degradation, hypoxia-induced down-regulation of FBXL14 may reduce c-Myc ubiquitination and degradation, which may up-regulate c-Myc protein levels to promote the maintenance of GSCs or facilitate the dedifferentiation of NSTCs to GSCs under hypoxia condition. In this study, we demonstrated that forced expression of FBXL14 promoted differentiation of GSCs and potently inhibited GSC tumor growth, suggesting a tumor-suppressive role of FBXL14 in GBM malignant growth.

In conclusion, we uncovered a ubiquitination and deubiquitination regulatory node of c-Myc in glioma cells and defined the role of this posttranslational regulation in cell fate determination of glioma cells. USP13 mediates ubiquitination of c-Myc to antagonize FBXL14-mediated ubiquitination and thus maintains the stem cell–like phenotype and tumorigenic potential of GSCs. As USP13 is preferentially expressed in GSCs relative to NSTCs and NPCs and disrupting USP13 reduced c-Myc protein and potently inhibited GSC proliferation and tumor growth, USP13 represents an attractive druggable target for developing a potential therapy to disrupt GSCs and effectively improve GBM treatment. In contrast, FBXL14 functions as a ubiquitin E3 ligase that targets c-Myc degradation through ubiquitination. Forced expression of FBXL14 induced GSC differentiation and inhibited tumor growth. Moreover, expression of the ubiquitination-insensitive T58A–c-Myc mutant rescued the inhibitory effects caused by USP13 disruption or FBXL14 overexpression. Thus, USP13 and FBXL14 play opposing roles in the regulation of the GSC phenotype through deubiquitination and ubiquitination of c-Myc. This regulatory balance represents a critical new paradigm in GSC fate determination and holds therapeutic promise as both a therapeutic target and prognostic marker.

## MATERIALS AND METHODS

### Isolation and characterization of glioma cells from GBMs

De-identified GBM surgical specimens were collected from the Cleveland Clinic Brain Tumor and Neuro-Oncology Center as well as the Brain Tumor and Neuro-Oncology Center at University Hospitals, Case Medical Center. The protocol for the collection and use of the human GBM surgical tumors for our study was approved by the Institutional Review Board. GSCs and matched NSTCs were isolated from primary GBM tumors or xenografts and functionally characterized as previously described (Bao et al., 2006a; Guryanova et al., 2011; Cheng et al., 2013; Zhou et al., 2015). In brief, glioma cells were dissociated from GBM tumors using the Papain Dissociation system (Worthington Biochemical Corporation). Glioma cells were labeled with an FITC-conjugated anti-CD15 antibody (347423; BD) and a PE-conjugated anti-CD133 antibody (130-090-854; Miltenyi Biotec) followed by FACS to isolate GSCs ($CD15^+/CD133^+$) and matched NSTCs ($CD15^-/CD133^-$). The sorted GSCs were maintained in Neurobasal medium (Invitrogen) supplemented with B-27 (Invitrogen), epidermal growth factor (EGF), and basic fibroblast growth factor (bFGF; 20 ng/ml each; R&D Systems). The cancer stem cell phenotypes of GSCs were validated by the expressions of GSC markers (SOX2, OLIG2, CD15, and L1CAM) and three functional assays (including in vitro limiting dilution assay, serum-induced cell differentiation assay, and in vivo tumorigenic assay) to assess the self-renewal potential, multilineage differentiation potency, and in vivo tumorigenic capacity of GSCs, as previously described (Bao et al., 2006a; Li et al., 2009; Guryanova et al., 2011; Cheng et al., 2013; Zhou et al., 2015).

### Culture of NPCs

Human NPC lines derived from fetal brains (Lonza) were cultured and maintained in suspension culture according to the vendor's instruction or propagated on stem cell Matrigel (BD). NPCs were kept in Neurobasal media (Invitrogen) supplemented with B27 (Invitrogen), EGF, and bFGF (20 ng/ml each; R&D Systems) as previously described (Guryanova et al., 2011; Huang et al., 2011).

### Identification of c-Myc–interacting proteins by mass spectrometry analysis

c-Myc–interacting proteins were coimmunoprecipitated from glioma cells and then analyzed by mass spectrometry. In brief, GSCs were transduced with Flag–c-Myc and then induced for partial differentiation by serum for a short time (2 d). The partially differentiated glioma cells expressing Flag–c-Myc or vector control were subjected to lysis in IP buffer. The c-Myc complexes were pulled down by two-step immunopurification (anti–Flag-M2 agarose and anti-Myc agarose), separated on SDS-PAGE, and visualized by silver staining. The gel pieces were then dehydrated in acetonitrile, dried in a speed vacuum, and digested with trypsin. The peptides were extracted from the polyacrylamide and were evaporated for liquid chromatography mass spectrometry (LC-MS) analysis.

### IB, immunofluorescence, and immunohistochemistry

IB analysis of protein expression and immunofluorescence staining on cells or tissue sections were performed as previously described (Bao et al., 2006a; Guryanova et al., 2011; Cheng et al., 2013; Zhou et al., 2015). Specific antibodies against USP13 (Abcam), c-Myc (Cell Signaling Technology or Santa Cruz Biotechnology, Inc.), SOX2 and OLIG2 (EMD Millipore or Santa Cruz Biotechnology, Inc.), Flag and α-tubulin (Sigma-Aldrich), GFAP (BioLegend or BD), MAP2 (Covance), TUJ1 (Covance), CD31 (Dako), FBXL14 (Santa Cruz Biotechnology, Inc.), CD133 (Miltenyi Biotec), ubiquitin (BioLegend), hemagglutinin (HA; Santa Cruz Biotechnology, Inc.), and Ki-67 (Abcam) were used for IB analysis or immunofluorescent staining. IHC staining on tumor and normal tissue sections was performed with an avidin–biotin complex kit and a 3,3′-diaminobenzine detection kit (Vector Laboratories) as previously described (Bao et al., 2006b; Guryanova et al., 2011; Zhou et al., 2015).

### IP

For IPs, GSCs or 293FT cells were lysed in the buffer (50 mM Hepes, 150 mM NaCl, 1% NP-40, and 5 mM EDTA) containing a protease inhibitor cocktail (Roche) and incubated with the indicated antibodies or antibody-conjugated agarose beads. Anti–Flag-M2 agarose and anti-Myc agarose beads were used to immunoprecipitate the indicated proteins from 293FT cells. Antibodies against FBXL14 (Santa Cruz Biotechnology, Inc.) and c-Myc (Cell Signaling Technology) in combination with protein A/G plus agarose (Santa Cruz Biotechnology, Inc.) were used to pull down the indicated proteins in GSC lysate.

### Ubiquitination assay

The ubiquitination assay was performed as previously described (Huang et al., 2011). Cells were treated with or without 10 μM MG132 for 6 h before they were collected. Co-IP of protein was performed as described in the previous section. The precipitated proteins were then released from the resins by boiling for 10 min in SDS-PAGE loading buffer. Then, the samples were subjected to Western blotting with the anti-ubiquitin antibody from BioLegend.

### Differentiation assay

GSCs were cultured on Matrigel-coated coverslips or dishes and then induced for differentiation by serum-containing medium (10% FBS in DMEM) or withdrawal of EGF and bFGF from neurobasal medium. At the indicated time points, cells were harvested for IB analysis or fixed for immunofluorescent staining of the indicated markers.

### DNA constructs, shRNAs, and lentivirus production

Lentiviral clones expressing USP13 shRNA (shUSP13), FBXL14 shRNA (shFBXL14), or shNT (SHC002) were acquired from Sigma-Aldrich. Two of five shUSP13 (shUSP13-50 and shUSP13-52) and two of five shFBXL14 (shFBXL14-1 and shFBXL14-2) that displayed high efficiency of knockdown (80–90% reduction) were used for all related experiments. Lentiviral constructs expressing Flag-tagged T58A–c-Myc (Flag-T58A-Myc), Flag-S62A-Myc, Flag-T58A-S62A-Myc, HA-tagged T58A–c-Myc (HA-T58A-Myc), Flag-tagged USP13 (Flag-USP13), and Flag-tagged USP13-C345A (Flag-USP13-C345A) were generated by cloning an open reading frame with the N-terminal Flag or HA sequence into the pCDH-MCS-T2A-Puro-MSCV vector (System Biosciences). Mutagenesis was done using a Quickchange Multi III Site-Directed Mutagenesis kit (Agilent Technologies) and confirmed by DNA sequencing. Viral particles were produced in 293T cells with the pACK set of helper plasmids (System Biosciences) in stem cell media. Viral stocks were concentrated by precipitation with PEG-8000 and titered according to the manufacturer's instructions.

### Apoptotic analysis by flow cytometry and TUNEL assay

Annexin V–FITC and propidium iodide (PI) staining was performed for flow cytometry according to the manufacturer's guidelines (BD). In brief, GSCs transduced with USP13 shRNA or shNT control for 48 h were washed in Neurobasal medium. Then, the cells were resuspended with 100 μl of binding buffer and incubated with 5 μl PI and 5 μl annexin V–FITC for 15 min in the dark at room temperature. Flow cytometric analysis was immediately performed using a flow cytometer (LSRII; BD). TUNEL assays detecting apoptotic cell death on tumor sections were performed with an ApopTag Plus Peroxidase In Situ Apoptosis kit (EMD Millipore) according to the manufacturer's instructions.

### Intracranial tumor formation and in vivo bioluminescent imaging

Intracranial transplantation of GSCs to establish GBM xenograft was performed as previously described (Bao et al., 2006a; Guryanova et al., 2011; Cheng et al., 2013; Zhou et al., 2015). To monitor tumor growth in living animals, all GSCs used for the animal study were transduced with firefly luciferase through lentiviral infection. GSCs expressing firefly luciferase were then transduced with shUSP13 or shNT, Flag-FBXL14 or vector, and/or Flag-T58A-Myc or vector control through lentiviral infection. 48 h after the lentiviral transduction, viable cells were intracranially transplanted into athymic immunocompromised mice. For the survival experiments, animals were maintained until manifestation of neurological signs or for 60 d. To examine the tumor growth, mouse brains implanted with GSCs were monitored by bioluminescent imaging or harvested simultaneously after GSC transplantation. Animals were administrated with D-luciferin intraperitoneally and anesthetized with isoflurane for the imaging analysis. The tumor luciferase images were captured by using an IVIS imaging system (Spectrum CT; PerkinElmer). All animal procedures were performed in accordance with Cleveland Clinic Institutional Animal Care and Use Committee–approved protocol.

### Inducible knockdown and overexpression

Inducible shUSP13 constructs (pTRIPZ-shUSP13; Tet-on) were purchased from Thermo Fisher Scientific. The inducible overexpression vector pCW was obtained from Addgene. The open reading frame of *FBXL14* with a Flag tag was inserted into pCW (NheI and BamHI) to construct a Tet-on pCW-Flag-FBXL14 overexpression that can be induced by doxycycline. GSCs stably expressing firefly luciferase were infected with lentivirus carrying inducible pTRIPZ-shUSP13 or pCW-Flag-FBXL14. The transduced cells were cultured in 0.5 µg/ml doxycycline for 3 d before cell lysates were collected to confirm inducible knockdown of USP13 or overexpression of FBXL14. After validation of inducible disruption or overexpression by doxycycline in vitro, GSCs were transplanted intracranially into immunocompromised mice supplied with water containing 2 mg/ml doxycycline or control water. Growth of orthotopic GBM tumors was monitored by bioluminescent imaging every 7 d.

### Quantitative RT-PCR

Total RNA was extracted with the RNeasy kit (QIAGEN) and reversely transcribed to cDNA with PrimeScript RT Master Mix (Takara Bio Inc.). Real-time PCR was performed on a cycler (Applied Biosystems) using SYBR green master mix (Invitrogen) with the following primers: *USP13*-F, 5′-CTAAATATGCCA ACAACCTCACCC-3′; *USP13*-R, 5′-GCCCGTTGCCCC CAGAGC-3′; *USP28*-F, 5′-TCCATGGAAATGCCTTCACA-3′; *USP28*-R, 5′-AATCTCACTCCTCCATCTCTGAAGAC-3′; *USP36*-F, 5′-AGCACTTTTCCCCCAGAACTG-3′; *USP36*-R, 5′-GGCTCCCAGATCTGCTGCTA-3′; USP37-F, 5′-GCCCAAAACAATCACAGAGC-3′; USP37-R, 5′-TCC CTTTCACGCTCCATATC-3′; *OTUB1*-F, 5′-TTTCTATCG GGCTTTCGGA-3′; *OTUB1*-R, 5′-TCGGAGGTGCTC TGGTCAT-3′; *FBXL14*-F, 5′-CCTGTGACAACATCAGTG ACAC-3′; *FBXL14*-R, 5′-GTTGATGCCATCATCACT GATG-3′; *FBW7*-F, 5′-ATGGGCCCTGCTCTTCACTTC ATGTCC-3′; *FBW7*-R, 5′-CACTGTGCGTTGTATGCA TC-3′; *RanBP2*-F, 5′-GAAATAAAACATTCTACACCGTC-3′; *RanBP2*-R, 5′-GTTTCAACTCCTGCATTTCTTTC-3′; *SKP2*-F, 5′-CCTAAGCAGCTGTTCCC-3′; *SKP2*-R, 5′-TTC GAGATACCCACAACCCC-3′; *UBR4*-F, 5′-GCTGCCCCA AACAGTGAAGAC-3′; and *UBR4*-R, 5′-GGTTTTGATAGC TGAGGCTTG-3′. The other primers were described previously (Fang et al., 2014).

### Statistical analysis

All grouped data are presented as mean ± SD. Difference between groups was assessed by one-way ANOVA or one-way ANOVA on rank tests. For the in vivo experiments, log-rank survival analysis was performed. SigmaStat Software (version 3.5; Systat Software, Inc.) was used for all statistical analyses.

## ACKNOWLEDGMENTS

We thank the Brain Tumor and Neuro-Oncology Centers at Cleveland Clinic and University Hospitals, Case Medical Center for providing GBM surgical specimens for this study. We are grateful to members in Dr. Rich's laboratory for scientific discussion. We also thank Cathy Shemo and Sage O'Bryant of the Flow Cytometry Core and J udith Drazba of the Imaging Core and Central Cell Services at Cleveland Clinic Lerner Research Institute for their assistance.

This work was supported by National Institutes of Health R01 grants (CA184090, NS091080, and NS099175) to S. Bao and a National Institutes of Health Shared Instrument Grant (S10OD018205) to the Cleveland Clinic Lerner Research Institute.

The authors declare no competing financial interests.

**Submitted: 23 October 2015**
**Revised: 20 July 2016**
**Accepted: 8 November 2016**

## REFERENCES

Abdelmoity, A.T., J.J. Hall, D.C. Bittel, and S. Yu. 2011. 1.39 Mb inherited interstitial deletion in 12p13.33 associated with developmental delay. *Eur. J. Med. Genet.* 54:198–203. http://dx.doi.org/10.1016/j.ejmg.2010.11.010

Adhikary, S., F. Marinoni, A. Hock, E. Hulleman, N. Popov, R. Beier, S. Bernard, M. Quarto, M. Capra, S. Goettig, et al. 2005. The ubiquitin ligase HectH9 regulates transcriptional activation by Myc and is essential for tumor cell proliferation. *Cell.* 123:409–421. http://dx.doi.org/10.1016/j.cell.2005.08.016

Annibali, D., J.R. Whitfield, E. Favuzzi, T. Jauset, E. Serrano, I. Cuartas, S. Redondo-Campos, G. Folch, A. Gonzàlez-Juncà, N.M. Sodir, et al. 2014. Myc inhibition is effective against glioma and reveals a role for Myc in proficient mitosis. *Nat. Commun.* 5:4632. http://dx.doi.org/10.1038/ncomms5632

Bao, S., Q. Wu, R.E. McLendon, Y. Hao, Q. Shi, A.B. Hjelmeland, M.W. Dewhirst, D.D. Bigner, and J.N. Rich. 2006a. Glioma stem cells promote radioresistance by preferential activation of the DNA damage response. *Nature.* 444:756–760. http://dx.doi.org/10.1038/nature05236

Bao, S., Q. Wu, S. Sathornsumetee, Y. Hao, Z. Li, A.B. Hjelmeland, Q. Shi, R.E. McLendon, D.D. Bigner, and J.N. Rich. 2006b. Stem cell-like glioma cells promote tumor angiogenesis through vascular endothelial growth factor. *Cancer Res.* 66:7843–7848. http://dx.doi.org/10.1158/0008-5472.CAN-06-1010

Bhatia, K., K. Huppi, G. Spangler, D. Siwarski, R. Iyer, and I. Magrath. 1993. Point mutations in the c-Myc transactivation domain are common in Burkitt's lymphoma and mouse plasmacytomas. *Nat. Genet.* 5:56–61. http://dx.doi.org/10.1038/ng0993-56

Blackwood, E.M., and R.N. Eisenman. 1991. Max: a helix-loop-helix zipper protein that forms a sequence-specific DNA-binding complex with Myc. *Science.* 251:1211–1217. http://dx.doi.org/10.1126/science.2006410

Calabrese, C., H. Poppleton, M. Kocak, T.L. Hogg, C. Fuller, B. Hamner, E.Y. Oh, M.W. Gaber, D. Finklestein, M. Allen, et al. 2007. A perivascular niche for brain tumor stem cells. *Cancer Cell.* 11:69–82. http://dx.doi.org/10.1016/j.ccr.2006.11.020

Charles, N.A., E.C. Holland, R. Gilbertson, R. Glass, and H. Kettenmann. 2012. The brain tumor microenvironment. *Glia.* 60:502–514. http://dx.doi.org/10.1002/glia.21264

Chen, J., Y. Li, T.S. Yu, R.M. McKay, D.K. Burns, S.G. Kernie, and L.F. Parada. 2012. A restricted cell population propagates glioblastoma growth after chemotherapy. *Nature.* 488:522–526. http://dx.doi.org/10.1038/nature11287

Chen, M., G.J. Gutierrez, and Z.A. Ronai. 2011. Ubiquitin-recognition protein Ufd1 couples the endoplasmic reticulum (ER) stress response to cell cycle control. *Proc. Natl. Acad. Sci. USA.* 108:9119–9124. http://dx.doi.org/10.1073/pnas.1100028108

Chen, R., M.C. Nishimura, S.M. Bumbaca, S. Kharbanda, W.F. Forrest, I.M. Kasman, J.M. Greve, R.H. Soriano, L.L. Gilmour, C.S. Rivers, et al. 2010. A hierarchy of self-renewing tumor-initiating cell types in glioblastoma. *Cancer Cell.* 17:362–375. http://dx.doi.org/10.1016/j.ccr.2009.12.049

Cheng, L., Z. Huang, W. Zhou, Q. Wu, S. Donnola, J.K. Liu, X. Fang, A.E. Sloan, Y. Mao, J.D. Lathia, et al. 2013. Glioblastoma stem cells generate vascular pericytes to support vessel function and tumor growth. *Cell.* 153:139–152. http://dx.doi.org/10.1016/j.cell.2013.02.021

Clague, M.J., and S. Urbé. 2010. Ubiquitin: same molecule, different degradation pathways. *Cell.* 143:682–685. http://dx.doi.org/10.1016/j.cell.2010.11.012

Cole, M.D., and V.H. Cowling. 2008. Transcription-independent functions of MYC: regulation of translation and DNA replication. *Nat. Rev. Mol. Cell Biol.* 9:810–815. http://dx.doi.org/10.1038/nrm2467

Dang, C.V. 2012. MYC on the path to cancer. *Cell.* 149:22–35. http://dx.doi.org/10.1016/j.cell.2012.03.003

David, C.J., M. Chen, M. Assanah, P. Canoll, and J.L. Manley. 2010. HnRNP proteins controlled by c-Myc deregulate pyruvate kinase mRNA splicing in cancer. *Nature.* 463:364–368. http://dx.doi.org/10.1038/nature08697

Delmore, J.E., G.C. Issa, M.E. Lemieux, P.B. Rahl, J. Shi, H.M. Jacobs, E. Kastritis, T. Gilpatrick, R.M. Paranal, J. Qi, et al. 2011. BET bromodomain inhibition as a therapeutic strategy to target c-Myc. *Cell.* 146:904–917. http://dx.doi.org/10.1016/j.cell.2011.08.017

Fang, X., Z. Huang, W. Zhou, Q. Wu, A.E. Sloan, G. Ouyang, R.E. McLendon, J.S. Yu, J.N. Rich, and S. Bao. 2014. The zinc finger transcription factor ZFX is required for maintaining the tumorigenic potential of glioblastoma stem cells. *Stem Cells.* 32:2033–2047. http://dx.doi.org/10.1002/stem.1730

Field, J.K., D.A. Spandidos, P.M. Stell, E.D. Vaughan, G.I. Evan, and J.P. Moore. 1989. Elevated expression of the c-myc oncoprotein correlates with poor prognosis in head and neck squamous cell carcinoma. *Oncogene.* 4:1463–1468.

Fontaine, J.F., D. Mirebeau-Prunier, M. Raharijaona, B. Franc, S. Triau, P. Rodien, O. Goëau-Brissonniére, L. Karayan-Tapon, M. Mello, R. Houlgatte, et al. 2009. Increasing the number of thyroid lesions classes in microarray analysis improves the relevance of diagnostic markers. *PLoS One.* 4:e7632. http://dx.doi.org/10.1371/journal.pone.0007632

Gao, P., I. Tchernyshyov, T.C. Chang, Y.S. Lee, K. Kita, T. Ochi, K.I. Zeller, A.M. De Marzo, J.E. Van Eyk, J.T. Mendell, and C.V. Dang. 2009. c-Myc suppression of miR-23a/b enhances mitochondrial glutaminase expression and glutamine metabolism. *Nature.* 458:762–765. http://dx.doi.org/10.1038/nature07823

Gargiulo, G., M. Cesaroni, M. Serresi, N. de Vries, D. Hulsman, S.W. Bruggeman, C. Lancini, and M. van Lohuizen. 2013. In vivo RNAi screen for BMI1 targets identifies TGF-β/BMP-ER stress pathways as key regulators of neural- and malignant glioma-stem cell homeostasis. *Cancer Cell.* 23:660–676. http://dx.doi.org/10.1016/j.ccr.2013.03.030

Gilbertson, R.J., and J.N. Rich. 2007. Making a tumour's bed: glioblastoma stem cells and the vascular niche. *Nat. Rev. Cancer.* 7:733–736. http://dx.doi.org/10.1038/nrc2246

Gordan, J.D., J.A. Bertout, C.J. Hu, J.A. Diehl, and M.C. Simon. 2007a. HIF-2α promotes hypoxic cell proliferation by enhancing c-myc transcriptional activity. *Cancer Cell.* 11:335–347. http://dx.doi.org/10.1016/j.ccr.2007.02.006

Gordan, J.D., C.B. Thompson, and M.C. Simon. 2007b. HIF and c-Myc: sibling rivals for control of cancer cell metabolism and proliferation. *Cancer Cell.* 12:108–113. http://dx.doi.org/10.1016/j.ccr.2007.07.006

Guryanova, O.A., Q. Wu, L. Cheng, J.D. Lathia, Z. Huang, J. Yang, J. MacSwords, C.E. Eyler, R.E. McLendon, J.M. Heddleston, et al. 2011. Nonreceptor tyrosine kinase BMX maintains self-renewal and tumorigenic potential of glioblastoma stem cells by activating STAT3. *Cancer Cell.* 19:498–511. http://dx.doi.org/10.1016/j.ccr.2011.03.004

Heddleston, J.M., Z. Li, J.D. Lathia, S. Bao, A.B. Hjelmeland, and J.N. Rich. 2010. Hypoxia inducible factors in cancer stem cells. *Br. J. Cancer.* 102:789–795. http://dx.doi.org/10.1038/sj.bjc.6605551

Hemmati, H.D., I. Nakano, J.A. Lazareff, M. Masterman-Smith, D.H. Geschwind, M. Bronner-Fraser, and H.I. Kornblum. 2003. Cancerous stem cells can arise from pediatric brain tumors. *Proc. Natl. Acad. Sci. USA.* 100:15178–15183. http://dx.doi.org/10.1073/pnas.2036535100

Hollern, D.P., I. Yuwanita, and E.R. Andrechek. 2013. A mouse model with T58A mutations in Myc reduces the dependence on KRas mutations and has similarities to claudin-low human breast cancer. *Oncogene.* 32:1296–1304. http://dx.doi.org/10.1038/onc.2012.142

Huang, Z., Q. Wu, O.A. Guryanova, L. Cheng, W. Shou, J.N. Rich, and S. Bao. 2011. Deubiquitylase HAUSP stabilizes REST and promotes maintenance of neural progenitor cells. *Nat. Cell Biol.* 13:142–152. http://dx.doi.org/10.1038/ncb2153

Jin, J., T. Cardozo, R.C. Lovering, S.J. Elledge, M. Pagano, and J.W. Harper. 2004. Systematic analysis and nomenclature of mammalian F-box proteins. *Genes Dev.* 18:2573–2580. http://dx.doi.org/10.1101/gad.1255304

Kim, J., M. Roh, I. Doubinskaia, G.N. Algarroba, I.E. Eltoum, and S.A. Abdulkadir. 2012. A mouse model of heterogeneous, c-MYC-initiated prostate cancer with loss of Pten and p53. *Oncogene.* 31:322–332. http://dx.doi.org/10.1038/onc.2011.236

King, B., T. Trimarchi, L. Reavie, L. Xu, J. Mullenders, P. Ntziachristos, B. Aranda-Orgilles, A. Perez-Garcia, J. Shi, C. Vakoc, et al. 2013. The ubiquitin ligase FBXW7 modulates leukemia-initiating cell activity by regulating MYC stability. *Cell.* 153:1552–1566. http://dx.doi.org/10.1016/j.cell.2013.05.041

Kozono, D., J. Li, M. Nitta, O. Sampetrean, D. Gonda, D.S. Kushwaha, D. Merzon, V. Ramakrishnan, S. Zhu, K. Zhu, et al. 2015. Dynamic epigenetic regulation of glioblastoma tumorigenicity through LSD1 modulation of MYC expression. *Proc. Natl. Acad. Sci. USA.* 112:E4055–E4064. http://dx.doi.org/10.1073/pnas.1501967112

Kreso, A., and J.E. Dick. 2014. Evolution of the cancer stem cell model. *Cell Stem Cell.* 14:275–291. http://dx.doi.org/10.1016/j.stem.2014.02.006

Lander, R., K. Nordin, and C. LaBonne. 2011. The F-box protein Ppa is a common regulator of core EMT factors Twist, Snail, Slug, and Sip1. *J. Cell Biol.* 194:17–25. http://dx.doi.org/10.1083/jcb.201012085

Lee, J., S. Kotliarova, Y. Kotliarov, A. Li, Q. Su, N.M. Donin, S. Pastorino, B.W. Purow, N. Christopher, W. Zhang, et al. 2006. Tumor stem cells derived from glioblastomas cultured in bFGF and EGF more closely mirror the phenotype and genotype of primary tumors than do serum-cultured cell lines. *Cancer Cell.* 9:391–403. http://dx.doi.org/10.1016/j.ccr.2006.03.030

Lewis, B.C., D.S. Klimstra, and H.E. Varmus. 2003. The c-myc and PyMT oncogenes induce different tumor types in a somatic mouse model for pancreatic cancer. *Genes Dev.* 17:3127–3138. http://dx.doi.org/10.1101/gad.1140403

Li, Z., S. Bao, Q. Wu, H. Wang, C. Eyler, S. Sathornsumetee, Q. Shi, Y. Cao, J. Lathia, R.E. McLendon, et al. 2009. Hypoxia-inducible factors regulate tumorigenic capacity of glioma stem cells. *Cancer Cell.* 15:501–513. http://dx.doi.org/10.1016/j.ccr.2009.03.018

Lin, C.Y., J. Lovén, P.B. Rahl, R.M. Paranal, C.B. Burge, J.E. Bradner, T.I. Lee, and R.A. Young. 2012. Transcriptional amplification in tumor cells with elevated c-Myc. *Cell.* 151:56–67. http://dx.doi.org/10.1016/j.cell.2012.08.026

Liu, G., X. Yuan, Z. Zeng, P. Tunici, H. Ng, I.R. Abdulkadir, L. Lu, D. Irvin, K.L. Black, and J.S. Yu. 2006. Analysis of gene expression and chemoresistance of $CD133^{+}$ cancer stem cells in glioblastoma. *Mol. Cancer.* 5:67. http://dx.doi.org/10.1186/1476-4598-5-67

Liu, J., H. Xia, M. Kim, L. Xu, Y. Li, L. Zhang, Y. Cai, H.V. Norberg, T. Zhang, T. Furuya, et al. 2011. Beclin1 controls the levels of p53 by regulating the deubiquitination activity of USP10 and USP13. *Cell.* 147:223–234. http://dx.doi.org/10.1016/j.cell.2011.08.037

Liu, Y., N. Soetandyo, J.G. Lee, L. Liu, Y. Xu, W.M. Clemons Jr., and Y. Ye. 2014. USP13 antagonizes gp78 to maintain functionality of a chaperone in ER-associated degradation. *eLife.* 3:e01369. http://dx.doi.org/10.7554/eLife.01369

Masui, K., K. Tanaka, D. Akhavan, I. Babic, B. Gini, T. Matsutani, A. Iwanami, F. Liu, G.R. Villa, Y. Gu, et al. 2013. mTOR complex 2 controls glycolytic metabolism in glioblastoma through FoxO acetylation and upregulation of c-Myc. *Cell Metab.* 18:726–739. http://dx.doi.org/10.1016/j.cmet.2013.09.013

Metzger, M.B., V.A. Hristova, and A.M. Weissman. 2012. HECT and RING finger families of E3 ubiquitin ligases at a glance. *J. Cell Sci.* 125:531–537. http://dx.doi.org/10.1242/jcs.091777

Nakayama, K.I., and K. Nakayama. 2006. Ubiquitin ligases: cell-cycle control and cancer. *Nat. Rev. Cancer.* 6:369–381. http://dx.doi.org/10.1038/nrc1881

Nie, Z., G. Hu, G. Wei, K. Cui, A. Yamane, W. Resch, R. Wang, D.R. Green, L. Tessarollo, R. Casellas, et al. 2012. c-Myc is a universal amplifier of expressed genes in lymphocytes and embryonic stem cells. *Cell.* 151:68–79. http://dx.doi.org/10.1016/j.cell.2012.08.033

Nieminen, A.I., J.I. Partanen, A. Hau, and J. Klefstrom. 2007. c-Myc primed mitochondria determine cellular sensitivity to TRAIL-induced apoptosis. *EMBO J.* 26:1055–1067. http://dx.doi.org/10.1038/sj.emboj.7601551

Pan, J., Q. Deng, C. Jiang, X. Wang, T. Niu, H. Li, T. Chen, J. Jin, W. Pan, X. Cai, et al. 2015. USP37 directly deubiquitinates and stabilizes c-Myc in lung cancer. *Oncogene.* 34:3957–3967. http://dx.doi.org/10.1038/onc.2014.327

Piccirillo, S.G., B.A. Reynolds, N. Zanetti, G. Lamorte, E. Binda, G. Broggi, H. Brem, A. Olivi, F. Dimeco, and A.L. Vescovi. 2006. Bone morphogenetic proteins inhibit the tumorigenic potential of human brain tumour-initiating cells. *Nature.* 444:761–765. http://dx.doi.org/10.1038/nature05349

Popov, N., M. Wanzel, M. Madiredjo, D. Zhang, R. Beijersbergen, R. Bernards, R. Moll, S.J. Elledge, and M. Eilers. 2007. The ubiquitin-specific protease USP28 is required for MYC stability. *Nat. Cell Biol.* 9:765–774. http://dx.doi.org/10.1038/ncb1601

Rahl, P.B., C.Y. Lin, A.C. Seila, R.A. Flynn, S. McCuine, C.B. Burge, P.A. Sharp, and R.A. Young. 2010. c-Myc regulates transcriptional pause release. *Cell.* 141:432–445. http://dx.doi.org/10.1016/j.cell.2010.03.030

Reyes-Turcu, F.E., J.R. Horton, J.E. Mullally, A. Heroux, X. Cheng, and K.D. Wilkinson. 2006. The ubiquitin binding domain ZnF UBP recognizes the C-terminal diglycine motif of unanchored ubiquitin. *Cell.* 124:1197–1208. http://dx.doi.org/10.1016/j.cell.2006.02.038

Saborowski, M., A. Saborowski, J.P. Morris IV, B. Bosbach, L.E. Dow, J. Pelletier, D.S. Klimstra, and S.W. Lowe. 2014. A modular and flexible ESC-based mouse model of pancreatic cancer. *Genes Dev.* 28:85–97. http://dx.doi.org/10.1101/gad.232082.113

Scortegagna, M., T. Subtil, J. Qi, H. Kim, W. Zhao, W. Gu, H. Kluger, and Z.A. Ronai. 2011. USP13 enzyme regulates Siah2 ligase stability and activity via noncatalytic ubiquitin-binding domains. *J. Biol. Chem.* 286:27333–27341. http://dx.doi.org/10.1074/jbc.M111.218214

Sears, R., F. Nuckolls, E. Haura, Y. Taya, K. Tamai, and J.R. Nevins. 2000. Multiple Ras-dependent phosphorylation pathways regulate Myc protein stability. *Genes Dev.* 14:2501–2514. http://dx.doi.org/10.1101/gad.836800

Singh, S.K., C. Hawkins, I.D. Clarke, J.A. Squire, J. Bayani, T. Hide, R.M. Henkelman, M.D. Cusimano, and P.B. Dirks. 2004. Identification of human brain tumour initiating cells. *Nature.* 432:396–401. http://dx.doi.org/10.1038/nature03128

Son, M.J., K. Woolard, D.H. Nam, J. Lee, and H.A. Fine. 2009. SSEA-1 is an enrichment marker for tumor-initiating cells in human glioblastoma. *Cell Stem Cell.* 4:440–452. http://dx.doi.org/10.1016/j.stem.2009.03.003

Stupp, R., W.P. Mason, M.J. van den Bent, M. Weller, B. Fisher, M.J. Taphoorn, K. Belanger, A.A. Brandes, C. Marosi, U. Bogdahn, et al. National Cancer Institute of Canada Clinical Trials Group. 2005. Radiotherapy plus concomitant and adjuvant temozolomide for glioblastoma. *N. Engl. J. Med.* 352:987–996. http://dx.doi.org/10.1056/NEJMoa043330

Stupp, R., M.E. Hegi, W.P. Mason, M.J. van den Bent, M.J. Taphoorn, R.C. Janzer, S.K. Ludwin, A. Allgeier, B. Fisher, K. Belanger, et al. National Cancer Institute of Canada Clinical Trials Group. 2009. Effects of radiotherapy with concomitant and adjuvant temozolomide versus radiotherapy alone on survival in glioblastoma in a randomised phase III study: 5-year analysis of the EORTC-NCIC trial. *Lancet Oncol.* 10:459–466. http://dx.doi.org/10.1016/S1470-2045(09)70025-7

Sun, X.X., X. He, L. Yin, M. Komada, R.C. Sears, and M.S. Dai. 2015. The nucleolar ubiquitin-specific protease USP36 deubiquitinates and stabilizes c-Myc. *Proc. Natl. Acad. Sci. USA.* 112:3734–3739. http://dx.doi.org/10.1073/pnas.1411713112

Suvà, M.L., E. Rheinbay, S.M. Gillespie, A.P. Patel, H. Wakimoto, S.D. Rabkin, N. Riggi, A.S. Chi, D.P. Cahill, B.V. Nahed, et al. 2014. Reconstructing and reprogramming the tumor-propagating potential of glioblastoma stem-like cells. *Cell.* 157:580–594. http://dx.doi.org/10.1016/j.cell.2014.02.030

Terunuma, A., N. Putluri, P. Mishra, E.A. Mathé, T.H. Dorsey, M. Yi, T.A. Wallace, H.J. Issaq, M. Zhou, J.K. Killian, et al. 2014. MYC-driven accumulation of 2-hydroxyglutarate is associated with breast cancer prognosis. *J. Clin. Invest.* 124:398–412. http://dx.doi.org/10.1172/JCI71180

Trent, J., P. Meltzer, M. Rosenblum, G. Harsh, K. Kinzler, R. Mashal, A. Feinberg, and B. Vogelstein. 1986. Evidence for rearrangement, amplification, and expression of c-myc in a human glioblastoma. *Proc. Natl. Acad. Sci. USA.* 83:470–473. http://dx.doi.org/10.1073/pnas.83.2.470

Varley, J.M., J.E. Swallow, W.J. Brammar, J.L. Whittaker, and R.A. Walker. 1987. Alterations to either c-erbB-2(neu) or c-myc proto-oncogenes in breast carcinomas correlate with poor short-term prognosis. *Oncogene.* 1:423–430.

Viñas-Castells, R., M. Beltran, G. Valls, I. Gómez, J.M. García, B. Montserrat-Sentís, J. Baulida, F. Bonilla, A.G. de Herreros, and V.M. Díaz. 2010. The hypoxia-controlled FBXL14 ubiquitin ligase targets SNAIL1 for proteasome degradation. *J. Biol. Chem.* 285:3794–3805. http://dx.doi.org/10.1074/jbc.M109.065995

von der Lehr, N., S. Johansson, S. Wu, F. Bahram, A. Castell, C. Cetinkaya, P. Hydbring, I. Weidung, K. Nakayama, K.I. Nakayama, et al. 2003. The F-box protein Skp2 participates in c-Myc proteosomal degradation and acts as a cofactor for c-Myc-regulated transcription. *Mol. Cell.* 11:1189–1200. http://dx.doi.org/10.1016/S1097-2765(03)00193-X

Wang, J., H. Wang, Z. Li, Q. Wu, J.D. Lathia, R.E. McLendon, A.B. Hjelmeland, and J.N. Rich. 2008. c-Myc is required for maintenance of glioma cancer stem cells. *PLoS One.* 3:e3769. http://dx.doi.org/10.1371/journal.pone.0003769

Wang, X., M. Cunningham, X. Zhang, S. Tokarz, B. Laraway, M. Troxell, and R.C. Sears. 2011. Phosphorylation regulates c-Myc's oncogenic activity in the mammary gland. *Cancer Res.* 71:925–936. http://dx.doi.org/10.1158/0008-5472.CAN-10-1032

Wasson, J.C., R.L. Saylors III, P. Zeltzer, H.S. Friedman, S.H. Bigner, P.C. Burger, D.D. Bigner, A.T. Look, E.C. Douglass, and G.M. Brodeur. 1990. Oncogene amplification in pediatric brain tumors. *Cancer Res.* 50:2987–2990.

Welcker, M., A. Orian, J. Jin, J.E. Grim, J.W. Harper, R.N. Eisenman, and B.E. Clurman. 2004. The Fbw7 tumor suppressor regulates glycogen synthase kinase 3 phosphorylation-dependent c-Myc protein degradation. *Proc. Natl. Acad. Sci. USA.* 101:9085–9090. http://dx.doi.org/10.1073/pnas.0402770101

Wen, P.Y., and S. Kesari. 2008. Malignant gliomas in adults. *N. Engl. J. Med.* 359:492–507. http://dx.doi.org/10.1056/NEJMra0708126

Yada, M., S. Hatakeyama, T. Kamura, M. Nishiyama, R. Tsunematsu, H. Imaki, N. Ishida, F. Okumura, K. Nakayama, and K.I. Nakayama. 2004. Phosphorylation-dependent degradation of c-Myc is mediated by the F-box protein Fbw7. *EMBO J.* 23:2116–2125. http://dx.doi.org/10.1038/sj.emboj.7600217

Yan, K., Q. Wu, D.H. Yan, C.H. Lee, N. Rahim, I. Tritschler, J. DeVecchio, M.F. Kalady, A.B. Hjelmeland, and J.N. Rich. 2014. Glioma cancer stem cells secrete Gremlin1 to promote their maintenance within the tumor hierarchy. *Genes Dev.* 28:1085–1100. http://dx.doi.org/10.1101/gad.235515.113

Yeh, E., M. Cunningham, H. Arnold, D. Chasse, T. Monteith, G. Ivaldi, W.C. Hahn, P.T. Stukenberg, S. Shenolikar, T. Uchida, et al. 2004. A signalling pathway controlling c-Myc degradation that impacts oncogenic transformation of human cells. *Nat. Cell Biol.* 6:308–318. http://dx.doi.org/10.1038/ncb1110

Yeh, H.M., C.Y. Yu, H.C. Yang, S.H. Ko, C.L. Liao, and Y.L. Lin. 2013. Ubiquitin-specific protease 13 regulates IFN signaling by stabilizing STAT1. *J. Immunol.* 191:3328–3336. http://dx.doi.org/10.4049/jimmunol.1300225

Zhang, J., P. Zhang, Y. Wei, H.L. Piao, W. Wang, S. Maddika, M. Wang, D. Chen, Y. Sun, M.C. Hung, et al. 2013. Deubiquitylation and stabilization of PTEN by USP13. *Nat. Cell Biol.* 15:1486–1494. http://dx.doi.org/10.1038/ncb2874

Zhang, Y.H., C.J. Zhou, Z.R. Zhou, A.X. Song, and H.Y. Hu. 2011. Domain analysis reveals that a deubiquitinating enzyme USP13 performs non-activating catalysis for Lys63-linked polyubiquitin. *PLoS One.* 6:e29362. http://dx.doi.org/10.1371/journal.pone.0029362

Zhao, X., B. Fiske, A. Kawakami, J. Li, and D.E. Fisher. 2011. Regulation of MITF stability by the USP13 deubiquitinase. *Nat. Commun.* 2:414. http://dx.doi.org/10.1038/ncomms1421

Zheng, H., H. Ying, H. Yan, A.C. Kimmelman, D.J. Hiller, A.J. Chen, S.R. Perry, G. Tonon, G.C. Chu, Z. Ding, et al. 2008. Pten and p53 converge on c-Myc to control differentiation, self-renewal, and transformation of normal and neoplastic stem cells in glioblastoma. *Cold Spring Harb. Symp. Quant. Biol.* 73:427–437. http://dx.doi.org/10.1101/sqb.2008.73.047

Zheng, H., Y. Du, Y. Hua, Z. Wu, Y. Yan, and Y. Li. 2012. Essential role of Fbxl14 ubiquitin ligase in regulation of vertebrate axis formation through modulating Mkp3 level. *Cell Res.* 22:936–940. http://dx.doi.org/10.1038/cr.2012.37

Zhou, W., S.Q. Ke, Z. Huang, W. Flavahan, X. Fang, J. Paul, L. Wu, A.E. Sloan, R.E. McLendon, X. Li, et al. 2015. Periostin secreted by glioblastoma stem cells recruits M2 tumour-associated macrophages and promotes malignant growth. *Nat. Cell Biol.* 17:170–182. http://dx.doi.org/10.1038/ncb3090